Main manuscript for:

Bacterial DNA on the skin surface overrepresents the viable skin microbiome

Authors: Ellen M Acosta[1], Katherine A Little[1], Benjamin P Bratton[1, 2, 3, 4], Jaime G Lopez[2], Xuming Mao[5], Aimee Payne[5], Mohamed S Donia[1], Danelle Devenport[1], Zemer Gitai[1*]

Affiliations:

[1] Department of Molecular Biology, Princeton University, Princeton, NJ 08544, USA.

[2] Lewis-Sigler Institute for Integrative Genomics, Princeton University, Princeton, NJ 08544, USA.

[3] Department of Pathology, Immunology and Microbiology, Vanderbilt University Medical Center, Nashville, TN 37232, USA

[4] Vanderbilt Institute for Infection, Immunology and Inflammation, Nashville, TN 37232, USA.

[5]Department of Dermatology, University of Pennsylvania, Philadelphia, PA 19104, USA.

***Correspondence to:** zgitai@princeton.edu

Author contributions: Conceptualization, Z.G., E.M.A., M.S.D,, and D.D.; Methodology, Z.G., E.M.A., and M.S.D. and D.D.; Software, E.M.A. J.G.L, and B.P.B.; Formal Analysis, E.M.A., J.G.L., and B.P.B.; Investigation, E.M.A., K.A.L., and X.M.; Resources, Z. G., D.D., and A.P.; Writing – Original Draft, Z.G. and E.M.A.; Writing – Reviewing & Editing, Z.G., E.M.A., B.P.B., D.D., and A.P.; Visualization, E.M.A. Z.G., and B.P.B.; Supervision, Z.G., D.D., and A.P.; Funding Acquisition, Z.G.

Competing interests: Authors declare no competing interests.

Classification: Biological science

Keywords: skin microbiome; 16S sequencing; fluorescence microscopy; bacterial viability

This PDF file includes:

Main text and figures

Materials and methods

References

Title: Bacterial DNA on the skin surface overrepresents the viable skin microbiome

Abstract

The skin microbiome provides vital contributions to human health. However, the spatial organization and viability of its bacterial components remain unclear. Here we apply culturing, imaging, and molecular approaches to human and mouse skin samples, and find that the skin surface is colonized by fewer viable bacteria than predicted by bacterial DNA levels. Instead, viable skin-associated bacteria are predominantly located in hair follicles and other cutaneous invaginations. Furthermore, we show that the skin microbiome has a uniquely low fraction of viable bacteria as compared to other human microbiome sites, indicating that most bacterial DNA on the skin surface is not associated with viable cells Additionally, a small number of bacterial families dominate each skin site and traditional sequencing methods overestimate both the richness and diversity of the skin microbiome. Finally, we performed an in-vivo skin microbiome perturbation-recovery study using human volunteers. Bacterial 16S rRNA gene sequencing revealed that, while the skin microbiome is remarkably stable even in the wake of aggressive perturbation, repopulation of the skin surface is driven by the underlying viable population. Our findings help explain the dynamics of skin microbiome perturbation, as bacterial DNA on the skin surface can be transiently perturbed but is replenished by a stable underlying viable population. These results address multiple outstanding questions in skin microbiome biology with significant implications for future efforts to study and manipulate it.

58 **Significance statement**

59 This study provides a crucial update to the skin microbiome paradigm by showing that viable
60 bacteria of the skin microbiome are primarily localized to hair follicles and other sub-cutaneous
61 structures rather than the skin surface. The native distribution of skin-associated bacteria has not
62 been previously evaluated, and here we show that the skin surface has few intact bacteria while
63 deeper structures are replete with bacterial contents. We used orthogonal approaches to evaluate
64 the source of bacterial DNA and the dynamics of bacterial repopulation on the skin surface to
65 develop an updated model of the skin microbiome. By adjusting the current understanding of the
66 skin microbiome to match this model, we will be able to address outstanding questions in the
67 field.

68

69

70

71

72

73

74

75

76

77

78

Main text

Introduction

The skin is the largest organ in the human body, providing roughly 25 square meters for potential host-microbe interactions (*1*). It facilitates our tactile interactions with the world, separates us from the dangers of our daily lives, and has the incredible ability to regenerate itself every 20-30 days (*2*). Human skin is also home to the organisms that comprise the skin microbiome, which has been shown to have important roles in human health. For example, the human skin microbiome affects immune system education (*3*, *4*), wound healing (*5*–*7*), colonization resistance (*8*), modulation of gene expression in the skin (*9*), and may have a role in development (*10*). Despite the many contributions of the skin microbiome to human health, there are important questions that have not been addressed by traditional methods: Why is the skin microbiome stable across months in longitudinal studies yet easily perturbed upon transient environmental changes like swimming (*11*)? Why are there so many anaerobic bacteria on an organ exposed to the air? And why is it so difficult to stably colonize the skin with new microbes without strong perturbations like abrasion? Traditional methods of sampling, culturing, and sequencing the bacterial members of the skin microbiome have been indispensable for establishing the skin microbiome field. Here, we extend these foundational studies with additional approaches to differentiate between viable and nonviable bacteria in order to begin to address these important questions.

Results

Fluorescence in-situ hybridization reveals few bacteria on the skin surface

101 The predominant method by which skin microbiomes have been studied is through
102 sequencing of DNA from swabbed skin areas (*12*). However, despite the fact that the skin
103 microbiome is often depicted as a well-mixed coating of microbes on the skin surface (*8*, *13*), it
104 remains unclear whether the DNA from the skin surface reflects the underlying biology of the
105 skin microbiome. Additionally, while sequencing and culture-based studies have demonstrated
106 that bacteria extend into deeper portions of the skin, the spatial distribution of the skin
107 microbiome as a whole has not been well characterized (*4*, *14*, *15*). To address this gap, we
108 determined the spatial distribution of bacterial cells in the skin using the universal bacterial FISH
109 probe EUB338, which hybridizes to bacterial 16S rRNA (*16*).

110 We first used EUB338 FISH on biopsied healthy adult human facial tissues and found
111 that the skin surface contains very few bacteria (Figure 1A). In contrast, clusters of bacteria were
112 found within hair follicles and other cutaneous skin structures like comedos (Figure 1B). There
113 are several possible explanations for the lack of FISH staining on the skin surface. For example,
114 viable surface bacteria may have been eliminated by sterilization of the biopsied area
115 (we address this possibility below). Alternatively, the surface bacteria could exist in a state like
116 stationary phase that has fewer EUB388-hybridizable ribosomes, or by skin microbiome
117 bacterial species being less prone to FISH probe hybridization. However, we confirmed that
118 EUB338 staining works well in stationary-phase cells of multiple skin microbiome bacterial
119 species (*Cutibacterium acnes, Staphylococcus epidermidis, Micrococcus luteus,* and
120 *Corynebacterium striatum*) (Figure 1 – figure supplement 1).

121 To quantify our FISH staining of human skin, we calculated the ratio of the mean
122 fluorescence within an area of interest (a hair follicle, the skin surface, or other cutaneous
123 structures) to the mean fluorescence outside of the area of interest. We refer to this ratio as an

enrichment score. The median enrichment score for human follicles was 11.24 (Figure 1D). In contrast, the skin surface (stratum corneum) had an enrichment score of just 0.188. This pattern of observing many bacteria in follicles but few on the skin surface held true when using FISH probes specific for *C. acnes*, one of the most abundant bacterial species in the human skin microbiome (Figure 1C). For *C. acnes*, the enrichment score was 3.14 for follicles as compared to 0.67 for the stratum corneum (Figure 1D). We note that while the majority of intact skin-associated bacteria were not associated with the skin surface, there are some visible bacteria on the skin surface, especially in areas near sub-surface structures (Figure 1A-B). This indicates that FISH staining is capable of detecting bacteria on the skin surface. Thus, our results are consistent with previous reports that bacteria can be cultured from skin surface swabs but also extend these findings to demonstrate that the skin surface has fewer intact bacteria than deeper skin structures.

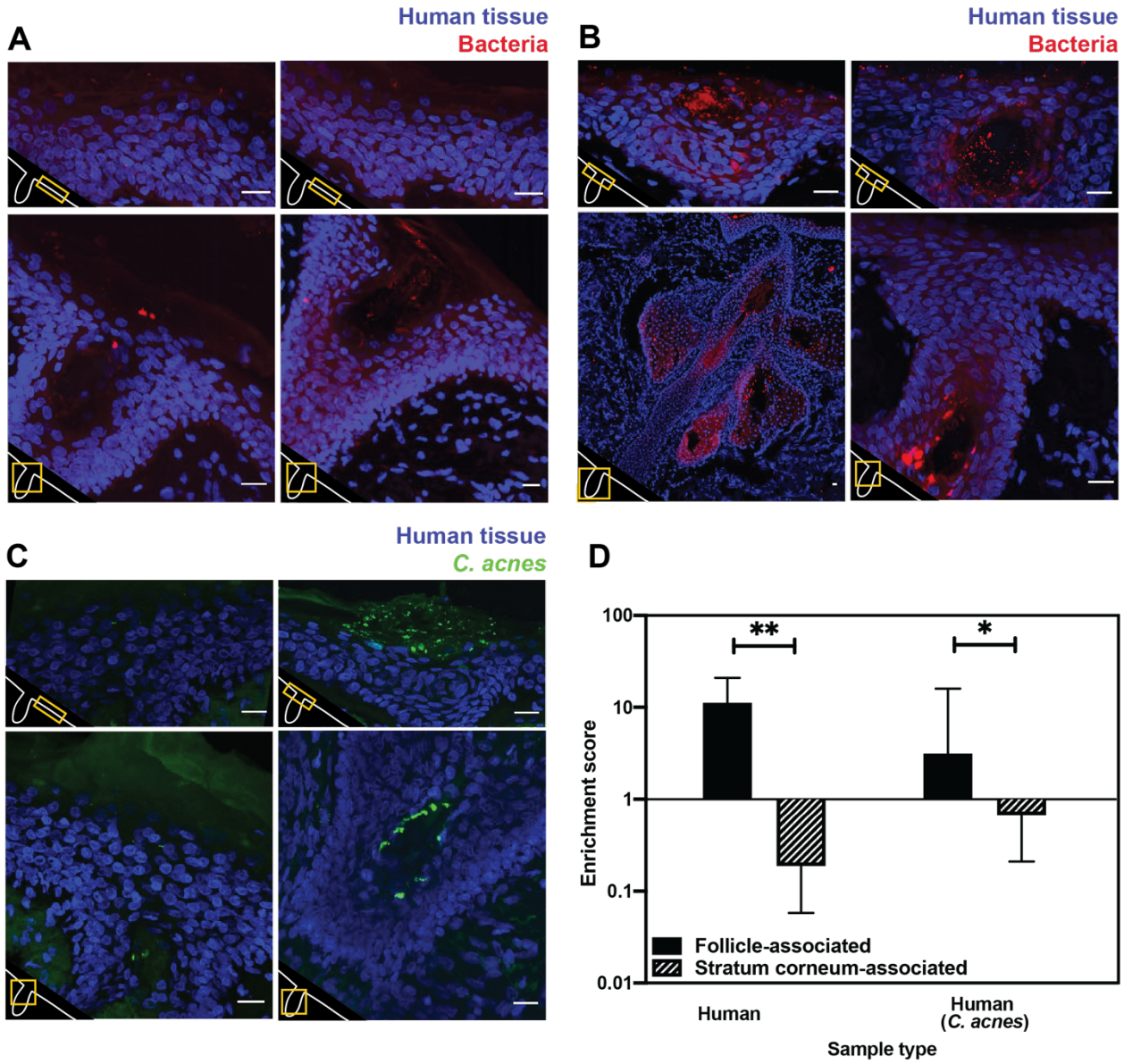

Figure 1: Bacterial FISH staining of human tissue. (A-C) Scale bar = 20 µm. The bottom left corner of each diagram shows a schematic of the hair follicle in white and the anatomic location of each image frame in yellow. DAPI staining is shown in blue in all parts. EUB338 hybridization is shown in red for all images. (A) Human tissues stained with the pan-bacterial FISH probe EUB338 show little bacterial presence at the skin surface. (B) Human tissues stained with EUB338 show abundant bacterial signal that is concentrated in hair follicles, pilosebaceous units, and other cutaneous structures. (C) Human tissues stained with a *C. acnes* specific FISH probe (in green) demonstrate the same overall spatial organization as those stained with EUB338. (D) Quantification enrichment scores showing the median and interquartile range. Significance was calculated using the Mann-Whitney test. *$P \leq 0.05$, **$P \leq 0.01$. N = 8 for human follicle, N = 6 for human follicle (*C. acnes*), N = 6 for human stratum corneum, N = 5 for human stratum corneum (*C. acnes*) where "N" represents different follicles or stratum corneum sections. The human tissue samples shown in Figure 1 were obtained from adult facial tissues (cheek and forehead).

151

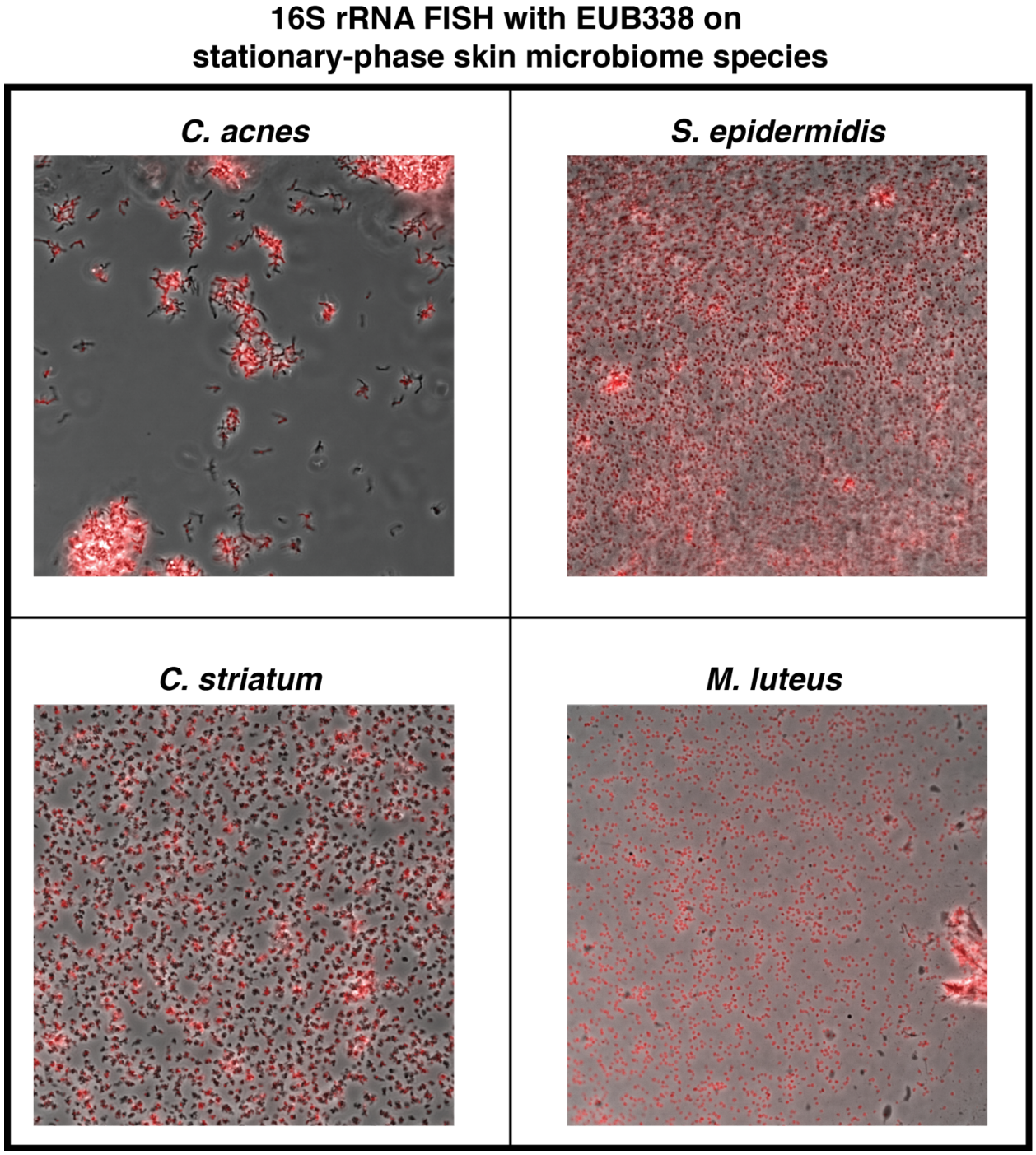

152
153 **Figure 1 – figure supplement 1**: **Fluorescence in situ hybridization on stationary-phase skin**
154 **microbiome bacterial species.** All bacterial species were grown in appropriate conditions to
155 stationary phase. The pan-bacterial FISH probe EUB338 was used. Hybridization is indicated in
156 red.

157 **Bacterial DNA on the skin surface overrepresents the number of viable bacteria**

158 DNA sequencing of samples collected by swabbing the skin surface is the most common
159 method used to evaluate the skin microbiome because it is simple, noninvasive, and has been
160 shown to result in higher consistency than other sampling methods (*17*). However, traditional
161 metagenomic and 16S rRNA gene sequencing do not differentiate DNA from viable and inviable
162 bacteria. We thus implemented a method that allowed us to quantitatively determine the fraction
163 of DNA in a sample that is specifically from intact bacteria. The ability to molecularly
164 differentiate between viable and inviable cells would enable us to both validate our FISH results
165 using an orthogonal method on untreated, living skin, and address the possibility that the low
166 numbers of intact surface bacteria observed by FISH was due to biopsy sterilization. To this end,
167 we utilized the cell-impermeable small molecule propidium monoazide (PMA), which binds
168 irreversibly to double-stranded DNA upon photoactivation to inhibit PCR amplification (Figure
169 2A) (*18*). When PMA photoactivation is performed before the cell lysis step of DNA isolation,
170 the genomic DNA inside viable bacteria is protected from PMA binding because PMA is cell-
171 impermeable, while cell-free DNA or DNA within permeabilized bacteria becomes PMA-bound.
172 To quantify bacterial DNA, we combined the use of PMA with droplet digital PCR (PMA-
173 ddPCR). Calculating the ratio of ddPCR counts between samples without PMA and samples with
174 PMA allowed us to generate a viability score for any given bacterial population. A similar
175 approach has been used to assess the viability of bacteria from environmental waste water
176 samples (*19*).

177 To assure that PMA-ddPCR would allow us to reliably gauge the fraction of viable cells
178 in a population, we first validated that it generated the expected results using known ratios of
179 either exponentially-growing or stationary-phase *E. coli* cultures combined with heat-killed *E.*

180 *coli* cells (Figure 2 – figure supplement 1A). To determine if PMA-ddPCR also works for skin-
181 resident bacterial species, we also applied PMA-ddPCR to four of the most common skin
182 microbiome bacteria, *S. epidermidis, C. acnes, M. luteus,* and *C. striatum.* We performed serial
183 dilutions of each bacterial culture and in parallel performed both CFU plating and ddPCR with or
184 without PMA. In every case, the amount of DNA in a sample (assessed by PMA-ddPCR)
185 correlated well with the number of culturable bacteria in high and low bacterial abundance
186 scenarios (Figure 2 – figure supplement 1B). Together, these controls confirm that PMA-ddPCR
187 is a reliable method for assessing the amount of DNA in a sample present within intact bacteria.
188 We next applied PMA-ddPCR to human skin microbiome samples by swabbing the skin
189 of four healthy human volunteers at eight sites (glabella, retroauricular crease, lower back, hair
190 shaft, antecubital fossa, popliteal fossa, nares, and dorsal forearm) (Figure 2B, Figure 2 – figure
191 supplement 2A, B). PMA-ddPCR revealed that the viability scores for these sites ranged between
192 0.02 and 0.12 (0 represents a fully-nonviable population, 1.0 represents a fully-viable
193 population), indicating that the majority of bacterial DNA found on the skin surface is not
194 associated with viable cells (Figure 2C). To investigate whether this was a skin-specific
195 phenomenon, we tested several non-skin microbiome sites (tongue, saliva, plaque, and feces).
196 We found that in all non-skin microbiome sites, the viability score was significantly higher than
197 for the skin, ranging from 0.4 (saliva) to 0.87 (feces) (Figure 2C).
198 We next sought to address whether our PMA-ddPCR viability scores accurately represent
199 of the number of viable bacteria on the skin surface. The low number of detectable bacteria on
200 the skin surface (either by FISH or PMA-ddPCR) does not imply that the skin surface is sterile
201 but rather that the majority of the bacterial DNA on the skin surface is not from these viable
202 cells. Indeed, culturing bacteria directly from the skin is common (*8*). To quantify the number of

203 viable bacteria directly, we plated a small amount of each sample using the standard conditions
204 for culturing skin microbes (5% sheep blood in tryptic soy agarose plates incubated both
205 aerobically and anaerobically). To determine whether PMA-ddPCR or traditional ddPCR better
206 represented the number of viable skin microbiome bacteria, we compared our results to a
207 standard curve generated with known numbers of *S. epidermidis.* For each sample, the PMA-
208 ddPCR quantification closely matched this standard curve while the samples lacking PMA
209 showed no overlap (Figure 2 – figure supplement 1C, D). The highest-abundance skin
210 microbiome species are readily culturable, such that quantifying the DNA from viable skin
211 surface bacteria should be able to accurately predict colony forming units (CFU) upon plating.
212 Quantifying the bacterial DNA in skin microbiome samples without the use of PMA resulted in
213 DNA quantities that were, on average, 82 times higher than predicted by the standard curve,
214 while the use of PMA brought this value down to just 1.3 (Figure 2 – figure supplement 1E).
215 Using ddPCR counts to predict CFU showed similar results, as ddPCR in the absence of PMA
216 yielded values that predicted CFU counts 58.5 times greater than those measured, while PMA-
217 ddPCR yielded values that predicted CFU counts that were on average only 1.28 times greater
218 than the actual cultured CFU (Figure 2 – figure supplement 1F). Since we expect a ratio near 1,
219 these findings lend further support for our conclusion that PMA-ddPCR reflects the viable
220 microbiome better than approaches lacking PMA.
221 Our FISH results from biopsied skin suggested that viable bacteria may be protected
222 below the skin surface. To test this hypothesis in untreated skin, we collected facial follicle
223 contents and used PMA-ddPCR to compare the viability of facial follicle contents and skin
224 surface samples (Figure 2D). The average viability for follicle contents was greater than 10-fold
225 higher for follicle contents than for the skin surface, confirming that cells in hair follicles are

226 more viable than those on the skin surface. Together, our results from FISH on biopsies and
227 PMA-ddPCR on skin swabs independently support the conclusion that the skin surface is
228 populated by few viable bacterial cells, indicating that the surface of healthy, non-sterilized
229 human skin is sparsely colonized. While these data indicate that bacterial DNA on the skin
230 surface is predominantly not associated with viable bacterial cells, we note that our results do not
231 suggest that there are no viable cells on the skin surface. Rather, our data indicate that the
232 majority of the bacterial DNA on the skin surface is not within bacteria such that using PMA
233 provides a much more accurate estimation of the viable skin microbiome.

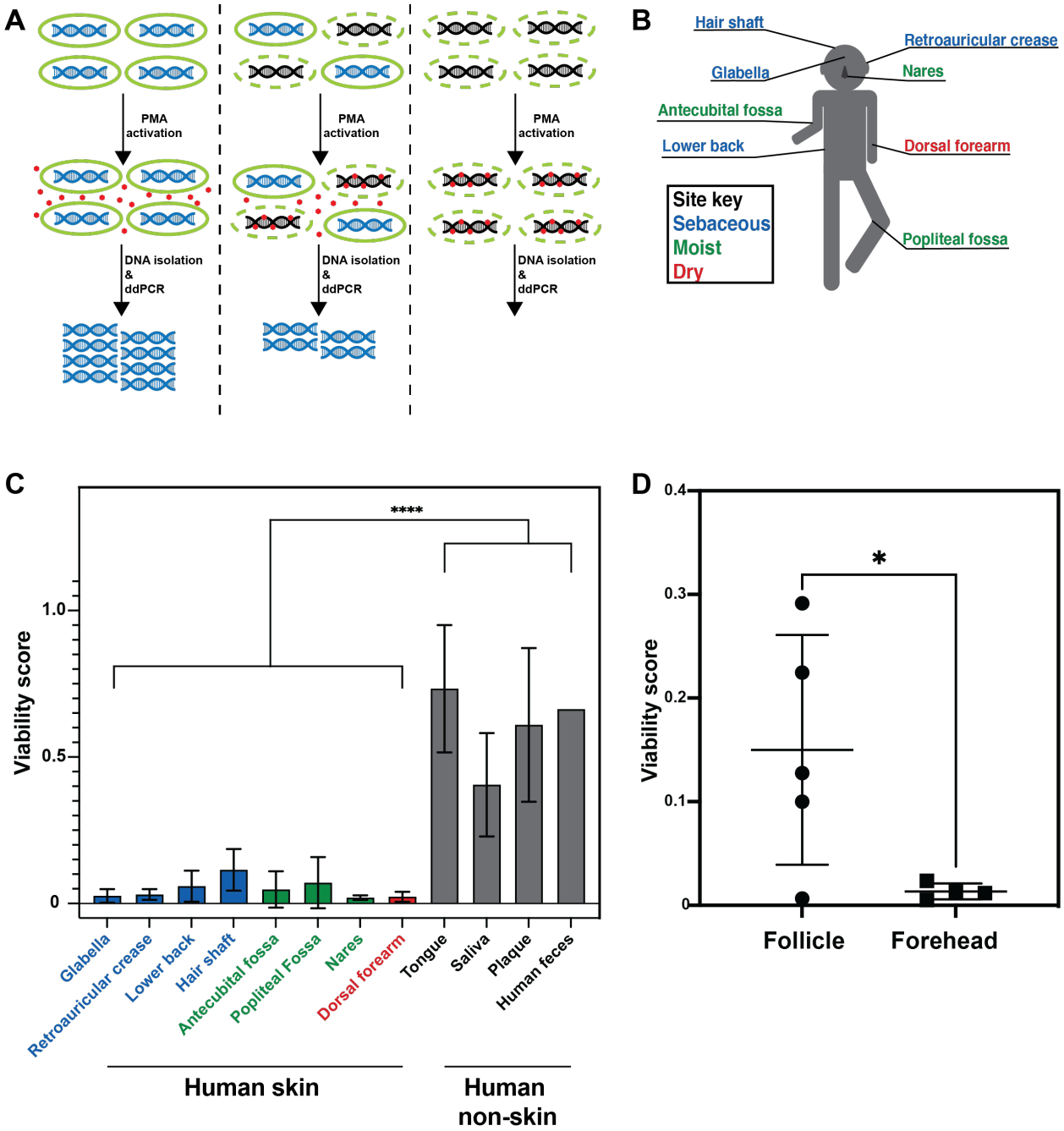

Figure 2: PMA-ddPCR and viability scores for human skin and non-skin microbiomes . (A) Schematic of the PMA-ddPCR workflow. (B) Sampling scheme showing each skin site that was sampled. Colors indicate site-type (sebaceous in blue, moist in green, dry in red). (C) PMA-ddPCR on skin and non-skin microbiome sites shows that the viability score of the skin microbiome is significantly lower than other microbiome sites. ****$P \leq 0.0001$ for Student's T Test on pooled skin and non-skin samples. Four volunteers contributed skin and non-skin microbiome samples. Additional samples were collected from some individuals and represent biological replicates. N= 8 for glabella, N = 6 for retroarticular crease, N = 5 for lower back, hair shaft, nares, and dorsal forearm, N = 3 for antecubital fossa, tongue, saliva, and plaque, N = 2 for popliteal fossa, and N = 1 for human feces. Each human skin sample site consists of samples

from four different individuals. Some volunteers were sampled multiple times on different days (at least two weeks apart). For glabella, one volunteer was sampled 4 times, one volunteer was sampled 2 times, and two volunteers were sampled 1 time. For retroauricular crease, two volunteers were sampled 2 times, and two volunteers were sampled 1 time. For lower back, one volunteer was sampled 2 times and three volunteers were sampled 1 time. For hair shaft, all samples came from one volunteer. For antecubital fossa, three volunteers were sampled 1 time. For popliteal fossa two volunteers were sampled 1 time. For nares, one volunteer was sampled 2 times and three volunteers were sampled 1 time. For dorsal forearm, one volunteer was sampled 2 times and three volunteers were sampled 1 time. Tongue, saliva, and plaque all represent 1 sample from three different individuals. For raw ddPCR counts, see Figure 2 – figure supplement 2A, B. (D) PMA-ddPCR on follicle contents and forehead swabs from 5 individuals. Mean viability score for follicle contents is 0.15 and for forehead is 0.013.

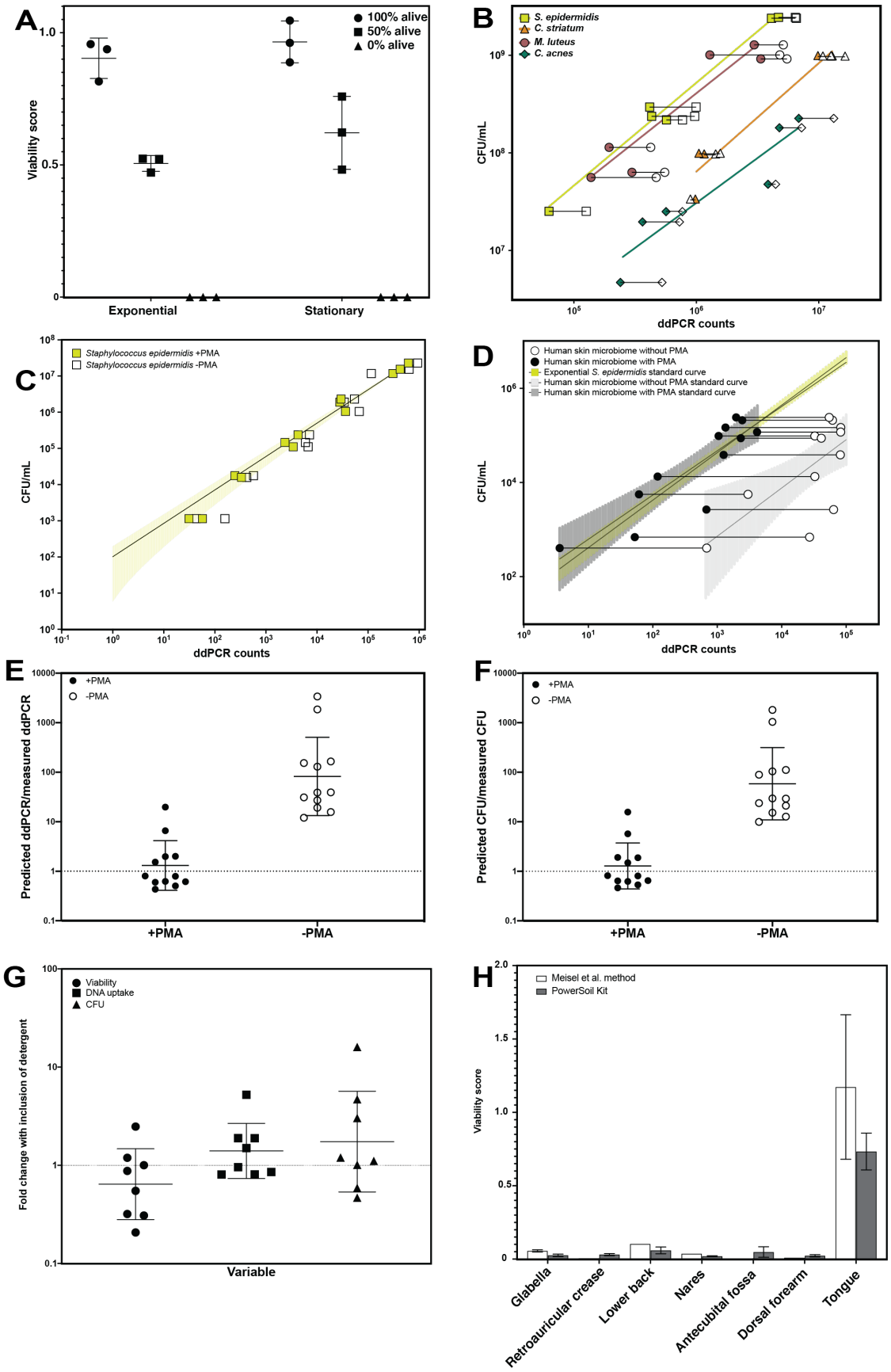
A
100% alive
50% alive
0% alive
Viability score
Exponential
Stationary
B
S. epidermidis
C. striatum
M. luteus
C. acnes
CFU/mL
ddPCR counts
C
Staphylococcus epidermidis +PMA
Staphylococcus epidermidis -PMA
CFU/mL
ddPCR counts
D
Human skin microbiome without PMA
Human skin microbiome with PMA
Exponential S. epidermidis standard curve
Human skin microbiome without PMA standard curve
Human skin microbiome with PMA standard curve
CFU/mL
ddPCR counts
E
+PMA
-PMA
Predicted ddPCR/measured ddPCR
+PMA
-PMA
F
+PMA
-PMA
Predicted CFU/measured CFU
+PMA
-PMA
G
Viability
DNA uptake
CFU
Fold change with inclusion of detergent
Variable
H
Meisel et al. method
PowerSoil Kit
Viability score
Glabella
Retroauricular crease
Lower back
Nares
Antecubital fossa
Dorsal forearm
Tongue

258

Figure 2 – figure supplement 1: PMA-ddPCR and sampling controls. (A) PMA-ddPCR validation controls on known ratios of heat-killed and exponentially-growing *E. coli* cultures. PMA-ddPCR performed on a population of exponentially-growing cells resulted in a viability score of 0.903,. PMA-ddPCR performed on a population of 100% heat-killed cells in exponential growth resulted in a viability score of 0. Populations consisting of 50% (by volume) heat-killed and 50% exponentially-growing cells exhibited an average viability score of 0.506. PMA-ddPCR performed on a population of stationary-phase cells resulted in a viability score of 0.965. PMA-ddPCR performed on a population of 100% heat-killed cells in stationary phase resulted in a viability score of 0. Populations consisting of 50% (by volume) heat-killed and 50% stationary-phase cells exhibited an average viability score of 0.621. Mean and standard deviation are shown. (B) Standard curves showing correlation between PMA-ddPCR counts and CFU for four skin microbiome bacterial species when grown to stationary phase. Open data points indicate samples without the use of PMA and closed data points indicate that PMA was used. Horizontal lines connect paired samples. (C) Standard curve showing correlation between PMA-ddPCR counts and CFU for exponentially-growing *Staphylococcus epidermidis*. 95% confidence interval is shown in the green shaded region. (D) Standard curve generated using *Staphylococcus epidermidis* cultures shown in green. Shading represents 95% confidence interval. Open and closed circles represent skin microbiome samples that did (closed circles) or did not (open circles) receive PMA treatment. Dark or light gray shading represents 95% confidence interval for skin microbiome samples. Paired samples are connected to show the downward shift in DNA abundance with the inclusion of PMA. (E) Comparison of the predicted ddPCR counts to measured ddPCR counts based on CFU for samples that were treated with PMA (closed circles) and samples that were not treated with PMA (open circles) (mean for PMA-treated samples is 1.31, mean for untreated samples is 82.2) . (F) Comparison of the predicted CFU to measured CFU based on ddPCR for samples that were treated with PMA (closed circles) and samples that were not treated with PMA (open circles) (mean for PMA treated samples is 1.28, mean for untreated samples is 58.5). (G) The effect of including 0.1% Triton X100 in swabbing buffer used for skin microbiome sampling. (H) Comparison of viability scores obtained with the two methods of DNA isolation used.

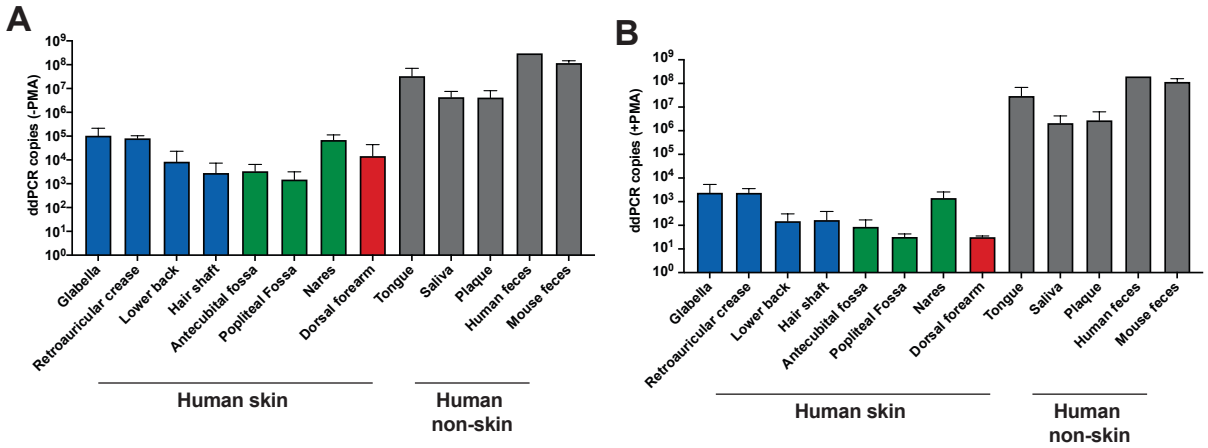

Figure 2 – figure supplement 2: Copies per 20 µL ddPCR reaction without (A) and with (B) the use of PMA. Data in A and B were used to calculate the viability score shown in Figure 2.

293 **Traditional sequencing methods overestimate skin microbiome richness and diversity**

294 Like many microbiomes, the existing knowledge of the skin microbiome is heavily based
295 upon bacterial 16S rRNA gene amplicon sequencing, which was developed to assess bacterial
296 populations while avoiding biases introduced by culturing methods. However, our findings
297 suggest that using 16S rRNA gene amplicon sequencing to study the skin microbiome is not
298 entirely unbiased, as most of the DNA in these samples is not from viable bacteria and traditional
299 16S rRNA gene amplicon sequencing does not differentiate between DNA originating from live
300 or dead cells. The inability of 16S rRNA gene amplicon sequencing to differentiate between
301 these two types of bacterial populations has been mentioned as a potential downfall of the
302 method (*8*). To evaluate how accurately traditional 16S rRNA gene amplicon sequencing
303 captures the living skin microbiome composition, we utilized PMA followed by 16S rRNA gene
304 amplicon sequencing (an approach we refer to as PMA-seq) (*20*). By sequencing pairs of
305 matched samples with PMA treatment (PMA-seq) and without PMA treatment (traditional
306 sequencing), we were able to explore how closely the microbiome compositions obtained from
307 traditional sequencing methods resembled the viable microbiome composition obtained by PMA-
308 seq (Figure 3A). These experiments established that at each skin site sampled, as compared to
309 traditional sequencing, the PMA-treated samples were less rich (richness, *R,* is a measure of the
310 number of identifiable bacterial taxa) and less diverse (diversity, *H,* is measured by the Shannon
311 diversity index) (Figure 3B, C). Furthermore, samples that had greater richness in traditional
312 sequencing (R_{trad}) showed proportionally larger decreases in richness and Shannon diversity with
313 PMA-seq (R_{PMA} and H_{PMA}) (Figure 3B, C). These results suggest that, although it appears by
314 traditional sequencing that there is a wide range of richness values at different skin sites (1-30
315 different taxa), in reality the richness across the skin microbiome at different body sites is

316 relatively similar and low (1-10 different taxa). Thus, though there appears to be a wide range of
317 diversity in the skin microbiome by traditional sequencing, PMA-seq indicates that this is
318 generally an overestimation at any given skin site. In fact, our results suggest that the viable skin
319 microbiome tends to be dominated by a relatively small number of taxa at most sites. An
320 independent analysis of glabella samples from 5 healthy volunteers including contamination
321 controls revealed the same trends that traditional sequencing overrepresented both diversity and
322 richness with or without contaminant removal (Figure 6 – figure supplement 3).

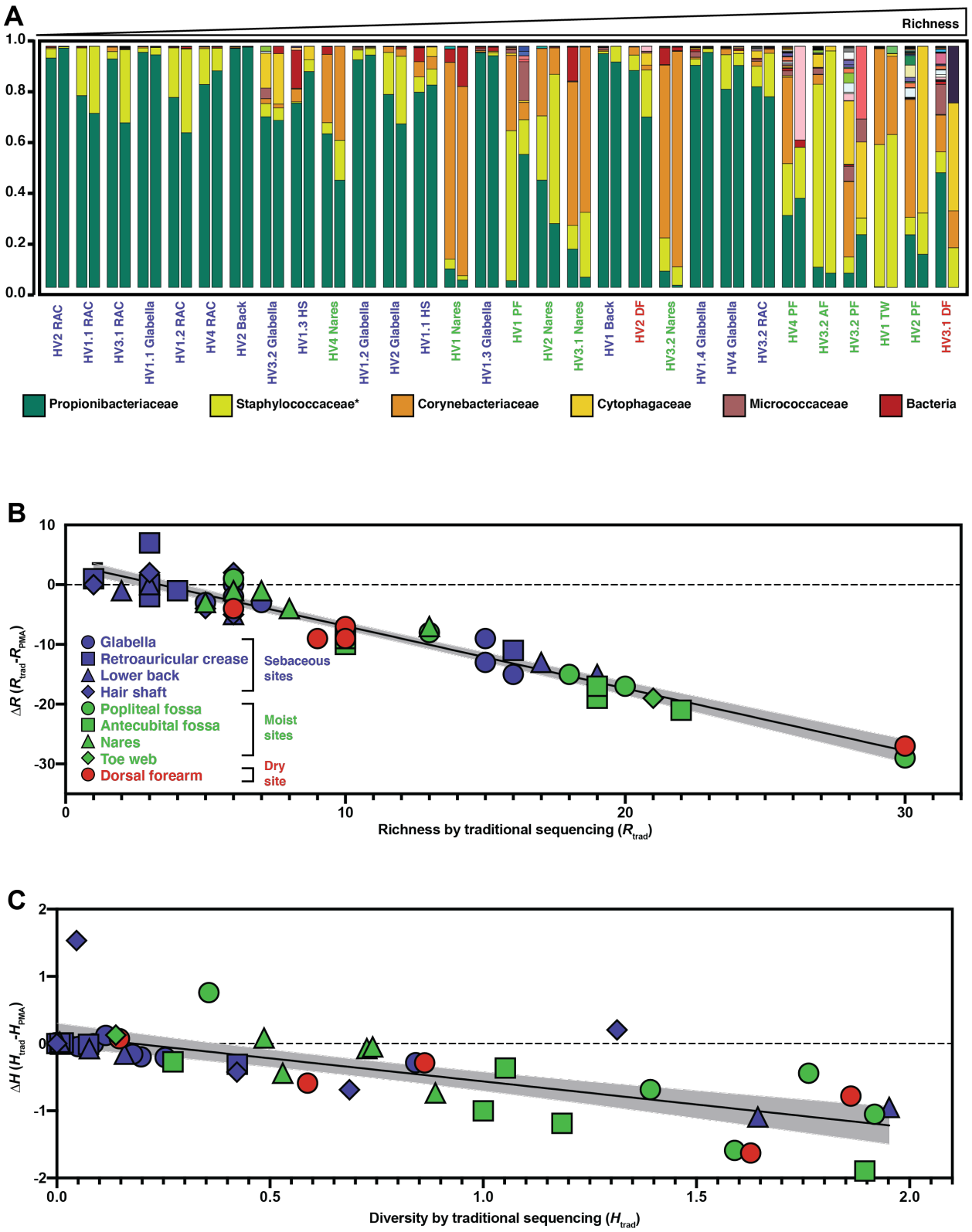

Figure 3: Relative abundance and change in richness and diversity of traditional sequencing compared to PMA-seq. (A) Relative abundance of all sequenced bacterial taxa at the family level. Paired bars represent data from traditional sequencing (left) and PMA-seq

327 (right). Samples are ordered by increasing richness in traditional sequencing. Labels below each
328 pair of bars indicate each sample's donor, replicate, and site (for example, HV1.1 RAC indicates
329 Healthy Volunteer 1, replicate sample 1, retroauricular crease). HS: hair shaft, RAC:
330 retroauricular crease, VF: volar forearm, PF: popliteal fossa, TW: toe web, AF: antecubital fossa.
331 *Relative abundance data for Staphylococcaceae was determined using forward-read sequencing
332 information only. Samples with fewer sequencing reads than PBS controls are not displayed. All
333 identified bacterial taxa with corresponding colors can be found in Figure 3 – figure supplement
334 1. (B) The richness changes between traditional sequencing (R_{trad}) and PMA-seq (R_{PMA}) are
335 demonstrated by plotting the change in richness (ΔR) against R_{trad}. Colors represent different site
336 types and shapes represent different sample sites. The shaded gray region represents the 95%
337 confidence interval for the linear regression. (C) The Shannon diversity changes between
338 traditional sequencing (H_{trad}) and PMA-seq (H_{PMA}) are demonstrated by plotting the change in
339 diversity (ΔH) against H_{trad}.

A

k__Bacteria.p__Actinobacteria.c__Actinobacteria.o__Actinomycetales.f__Propionibacteriaceae
k__Bacteria;p__Firmicutes;c__Bacilli;o__Bacillales;f__Staphylococcaceae
k__Bacteria.p__Actinobacteria.c__Actinobacteria.o__Actinomycetales.f__Corynebacteriaceae
k__Bacteria.p__Bacteroidetes.c__Cytophagia.o__Cytophagales.f__Cytophagaceae
k__Bacteria.p__Actinobacteria.c__Actinobacteria.o__Actinomycetales.f__Micrococcaceae
k__Bacteria.__.__.__.__
k__Bacteria.p__Proteobacteria.c__Alphaproteobacteria.o__Sphingomonadales.f__Sphingomonadaceae
k__Bacteria.p__Actinobacteria.c__Actinobacteria.o__Actinomycetales.f__Intrasporangiaceae
k__Bacteria.p__Proteobacteria.c__Alphaproteobacteria.o__Rickettsiales.f__
k__Bacteria.p__Actinobacteria.c__Actinobacteria.o__Actinomycetales.f__Nocardiaceae
k__Bacteria.p__Proteobacteria.c__Alphaproteobacteria.o__Rhodobacterales.f__Rhodobacteraceae
k__Bacteria.p__Proteobacteria.c__Alphaproteobacteria.o__Rhizobiales.f__Hyphomicrobiaceae
k__Bacteria.p__Proteobacteria.c__Alphaproteobacteria.o__Rhizobiales.f__Rhizobiaceae
k__Bacteria.p__Actinobacteria.c__Actinobacteria.o__Actinomycetales.f__Microbacteriaceae
k__Bacteria.p__Actinobacteria.c__Actinobacteria.o__Actinomycetales.f__Nocardioidaceae
k__Bacteria.p__Actinobacteria.c__Actinobacteria.o__Actinomycetales.f__Dietziaceae
k__Bacteria.p__Actinobacteria.c__Actinobacteria.o__Actinomycetales.f__Dermabacteraceae
k__Bacteria.p__Proteobacteria.c__Alphaproteobacteria.o__Rhizobiales.f__Methylobacteriaceae
k__Bacteria.p__TM7.c__TM7.3.o__EW055.f__
k__Bacteria.p__Cyanobacteria.c__Chloroplast.o__Stramenopiles.f__
k__Bacteria.p__Actinobacteria.c__Actinobacteria.o__Actinomycetales.f__Mycobacteriaceae
k__Bacteria.p__Actinobacteria.c__Actinobacteria.o__Actinomycetales.__
k__Bacteria.p__Actinobacteria.c__Actinobacteria.o__Actinomycetales.f__Brevibacteriaceae
k__Bacteria.p__Proteobacteria.c__Alphaproteobacteria.o__Rhizobiales.f__Bradyrhizobiaceae
k__Bacteria.p__Actinobacteria.c__Actinobacteria.o__Actinomycetales.f__Gordoniaceae
k__Bacteria.p__Thermi..c__Deinococci.o__Deinococcales.f__Deinococcaceae
k__Bacteria.p__Fusobacteria.c__Fusobacteriia.o__Fusobacteriales.f__Fusobacteriaceae
k__Bacteria.p__Proteobacteria.c__Alphaproteobacteria.o__Caulobacterales.f__Caulobacteraceae
k__Bacteria.p__Firmicutes.c__Clostridia.o__Clostridiales.f__Clostridiaceae
k__Bacteria.p__Chloroflexi.c__Thermomicrobia.o__JG30.KF.CM45.f__
k__Bacteria.p__Proteobacteria.c__Alphaproteobacteria.o__Rhizobiales.f__Aurantimonadaceae
k__Bacteria.p__Thermi..c__Deinococci.o__Thermales.f__Thermaceae
k__Bacteria.p__Firmicutes.c__Clostridia.o__Clostridiales.f__Ruminococcaceae
k__Bacteria.p__Proteobacteria.c__Alphaproteobacteria.o__Rhizobiales.f__Xanthobacteraceae
k__Bacteria.p__Actinobacteria.c__Actinobacteria.o__Actinomycetales.f__Pseudonocardiaceae
k__Bacteria.p__Actinobacteria.c__Actinobacteria.o__Actinomycetales.f__Nakamurellaceae
k__Bacteria.p__Proteobacteria.__.__.__
k__Bacteria.p__Proteobacteria.c__Epsilonproteobacteria.o__Campylobacterales.f__Campylobacteraceae
k__Bacteria.p__Proteobacteria.c__Alphaproteobacteria.o__Rhodospirillales.f__Acetobacteraceae
k__Bacteria.p__Fusobacteria.c__Fusobacteriia.o__Fusobacteriales.f__Leptotrichiaceae
k__Bacteria.p__Proteobacteria.c__Alphaproteobacteria.o__Rhodospirillales.f__Rhodospirillaceae
k__Bacteria.p__Proteobacteria.c__Alphaproteobacteria.o__Rickettsiales.f__mitochondria
k__Bacteria.p__Proteobacteria.c__Alphaproteobacteria.o__Rhizobiales.__
k__Bacteria.p__Acidobacteria.c__Acidobacteria.5.o__.f__
k__Bacteria.p__Actinobacteria.c__Actinobacteria.o__Actinomycetales.f__Williamsiaceae
k__Bacteria.p__TM7.c__TM7.3.o__.f__
k__Bacteria.p__Firmicutes.c__Clostridia.o__Clostridiales.f__Peptostreptococcaceae
k__Bacteria.p__Bacteroidetes.c__Flavobacteriia.o__Flavobacteriales.f__Flavobacteriaceae
k__Bacteria.p__Firmicutes.c__Bacilli.o__Bacillales.f__Thermoactinomycetaceae
k__Bacteria.p__Actinobacteria.c__Actinobacteria.o__Actinomycetales.f__Promicromonosporaceae
k__Bacteria.p__Firmicutes.c__Bacilli.o__Bacillales.f__Staphylococcaceae
k__Bacteria.p__Actinobacteria.c__Actinobacteria.o__Actinomycetales.f__Tsukamurellaceae
k__Bacteria.p__Proteobacteria.c__Alphaproteobacteria.o__Sphingomonadales.f__Erythrobacteraceae
k__Bacteria.p__Actinobacteria.c__Acidimicrobiia.o__Acidimicrobiales.f__
k__Bacteria.p__Proteobacteria.c__Alphaproteobacteria.o__BD7.3.f__
k__Bacteria.p__Actinobacteria.c__Actinobacteria.o__Actinomycetales.f__Geodermatophilaceae
k__Bacteria.p__Actinobacteria.c__Actinobacteria.o__Actinomycetales.f__Micromonosporaceae
k__Bacteria.p__Chloroflexi.c__Chloroflexi.o__.Roseiflexales..f__.Kouleothrixaceae.
k__Bacteria.p__Actinobacteria.c__Actinobacteria.o__Actinomycetales.f__Dermacoccaceae
k__Bacteria.p__Actinobacteria.c__Actinobacteria.o__Actinomycetales.f__Sporichthyaceae
k__Bacteria.p__Cyanobacteria.__.__.__
k__Bacteria.p__Firmicutes.c__Clostridia.o__Clostridiales.__
k__Bacteria.p__Proteobacteria.c__Alphaproteobacteria.__.__
k__Bacteria.p__Firmicutes.c__Clostridia.o__Clostridiales.f__
k__Bacteria.p__Firmicutes.c__Clostridia.o__Clostridiales.f__.Tissierellaceae.
k__Bacteria.p__Actinobacteria.c__Actinobacteria.o__Actinomycetales.f__Thermomonosporaceae
k__Bacteria.p__Actinobacteria.c__Actinobacteria.o__Actinomycetales.f__
k__Bacteria.p__Acidobacteria.c__.Chloracidobacteria..o__RB41.f__Ellin6075
k__Bacteria.p__Proteobacteria.c__Betaproteobacteria.__.__
k__Bacteria.p__SR1.c__.o__.f__
k__Bacteria.p__Actinobacteria.c__Acidimicrobiia.o__Acidimicrobiales.f__C111
k__Bacteria.p__WPS.2.c__.o__.f__
k__Bacteria.p__Cyanobacteria.c__Chloroplast.o__.f__
k__Bacteria.p__Proteobacteria.c__Alphaproteobacteria.o__Rhizobiales.f__Methylocystaceae
k__Bacteria.p__Actinobacteria.c__Acidimicrobiia.o__Acidimicrobiales.f__EB1017
k__Bacteria.p__Planctomycetes.c__Phycisphaerae.o__WD2101.f__
k__Bacteria.p__Proteobacteria.c__Alphaproteobacteria.o__Rhizobiales.f__Brucellaceae
k__Bacteria.p__Gemmatimonadetes.c__Gemmatimonadetes.o__Gemmatimonadales.f__Ellin5301
k__Bacteria.p__Actinobacteria.c__Coriobacteriia.o__Coriobacteriales.f__Coriobacteriaceae
k__Bacteria.p__Actinobacteria.c__Actinobacteria.o__Actinomycetales.f__Cellulomonadaceae
k__Bacteria.p__Actinobacteria.c__Actinobacteria.o__Actinomycetales.f__Kineosporiaceae
k__Bacteria.p__Proteobacteria.c__Alphaproteobacteria.o__Rhizobiales.f__Beijerinckiaceae
k__Bacteria.p__Cyanobacteria.c__Chloroplast.o__Streptophyta.f__
k__Bacteria.p__Proteobacteria.c__Alphaproteobacteria.o__Rhizobiales.f__Phyllobacteriaceae
k__Bacteria.p__.c__.o__.f__
k__Bacteria.p__Cyanobacteria.c__Oscillatoriophycideae.o__Oscillatoriales.f__Phormidiaceae
k__Bacteria.p__OD1.c__.o__.f__
k__Bacteria.p__Proteobacteria.c__Betaproteobacteria.o__Neisseriales.f__Neisseriaceae
k__Bacteria.p__OD1.c__ZB2.o__.f__
k__Bacteria.p__Chloroflexi.c__Anaerolineae.o__Ardenscatenales.f__Ardenscatenaceae
k__Bacteria.p__Proteobacteria.c__Alphaproteobacteria.o__Rhizobiales.f__Bartonellaceae
k__Bacteria.p__Firmicutes.c__Bacilli.o__Lactobacillales.f__Streptococcaceae
k__Bacteria.p__GN02.c__BD1.5.o__.f__

Figure 3 – figure supplement 1: Full list of identified taxa with corresponding colors. (A) Full list of identified bacterial groups shown in Figure 3.

343 **Most bacterial groups are overrepresented by traditional sequencing methods**

344 The metrics of richness and diversity offer important information regarding how the
345 composition of the skin microbiome changes at different body sites between traditional
346 sequencing and PMA-seq. We further wanted to understand the changes in the relative
347 abundance of specific bacterial taxa. To quantify taxon-level PMA-dependent changes, we
348 developed a PMA-index (I_{PMA}) for each bacterial taxon, which is calculated as follows:
349 $I_{PMA}=\frac{A_{PMA}}{(A_{PMA})+(A_{trad})}$, where A_{PMA} is the relative abundance by PMA-seq and A_{trad} is the relative
350 abundance by traditional sequencing. A low PMA-index (below 0.5) indicates that the taxon in
351 question is overrepresented by traditional sequencing, while a high PMA index (above 0.5)
352 indicates that the taxon in question is underrepresented by traditional sequencing (Figure 4A).
353 We note that these values represent enrichment relative to the rest of the sequences, a
354 measurement that is distinct from the viability score. Calculating PMA-indices revealed that the
355 abundances of most bacterial taxa at any given body site are overestimated by traditional
356 sequencing, as most taxa had PMA-index values close to 0 (Figure 4A). 16S rRNA copy
357 numbers could affect these values but the 16S copy numbers of the most abundant species were
358 all within a roughly two-fold range, such that this effect is minor compared to the trends
359 observed (*21*).

360 The four most abundant bacterial families (*Propionibacteriaceae*, *Staphylococcaceae,*
361 *Corynebacteriaceae*, and *Micrococcaceae*) made up 93% of total sequencing reads (96% of
362 PMA-seq reads and 91% of traditional sequencing reads) and demonstrated interesting family-
363 level PMA-index patterns. The family *Propionibacteriaceae* includes a major component of the
364 skin microbiome*, C. acnes*, which has been shown by traditional sequencing to comprise
365 upwards of 50% of the skin microbiome irrespective of site type (*8*). PMA-seq revealed that

366 traditional sequencing accurately represents *Propionibacteriaceae* abundance in sebaceous sites
367 (demonstrated by a PMA-index close to 0.5), but overrepresents *Propionibacteriaceae* in moist
368 and dry sites (PMA-indices of 0.2-0.3). Furthermore, *Propionibacteriaceae* dominated sebaceous
369 sites (accounting for >75% of all viable bacteria in most sebaceous samples), but did not
370 dominate moist or dry sites (their viable abundance did not exceed 50% of all viable bacteria in
371 any of those samples) (Figure 4 A, B). Similar to the *Propionibacteriaceae,* bacteria in the
372 family *Staphylococcaceae* appeared to be well-represented across all body sites (Figure 4A, B
373 and Figure 4 – figure supplement 2).

374 Bacteria in the family *Corynebacteriaceae* are also considered main constituents of the
375 skin microbiome, but our results showed that traditional sequencing overestimates the abundance
376 of *Corynebacteriaceae* at every skin site except for the nares. For example, traditional
377 sequencing identified a high abundance of *Corynebacteriaceae* in the popliteal fossa, but PMA-
378 seq showed that these reads were largely of inviable origin (Figure 4B). Previous studies have
379 demonstrated that *Corynebacteria* are readily cultured from nasal isolates, which supports our
380 PMA-seq finding that viable members of this taxon are abundant in the nares but not at most
381 other skin sites (*22*).

382 Interestingly, *Micrococcaceae* were overrepresented by traditional sequencing at every
383 site except for the hair shaft. In the hair shaft, *Micrococcaceae* were abundant by PMA-seq but
384 almost undetectable by traditional sequencing. As shown in Figure 4B, the increase in the
385 relative proportion of viable *Micrococcaceae* detected by PMA-seq corresponds to a decrease in
386 viable *Propionibacteriaceae*, suggesting that *Micrococcaceae* may not be detected by traditional
387 sequencing because of the high abundance of DNA from inviable *Propionibacteriaceae.* These
388 results suggest that most skin sites are colonized by a relatively small number of bacterial

389 families, that different families distinctly colonize different skin sites, and that the majority of the

390 additional bacterial DNA on the skin surface comes from inviable bacteria.

391

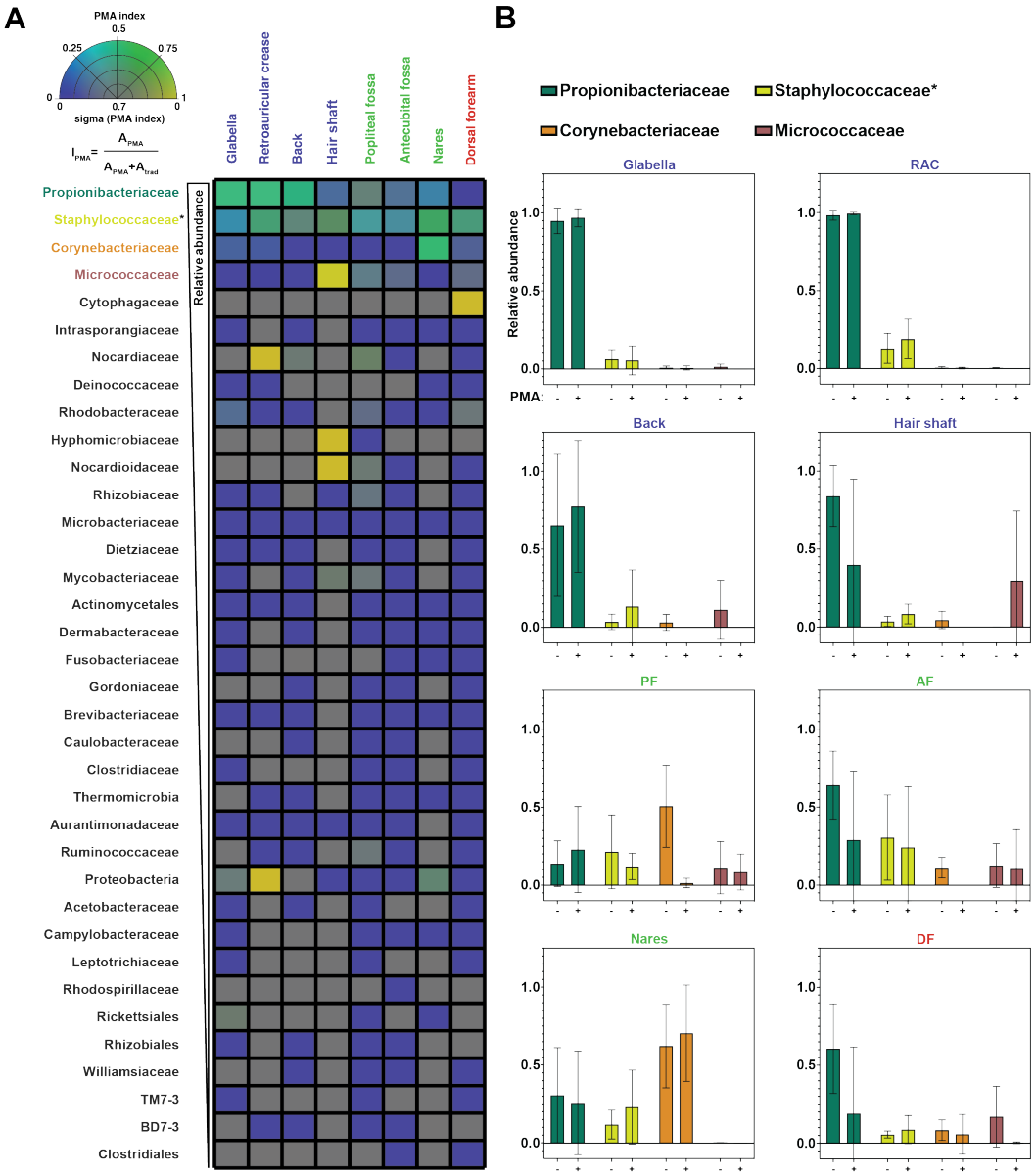

Figure 4: PMA-index and change in relative abundance between traditional and PMA-seq. (A) The PMA index for each bacterial taxon that was present in at least 4 samples is shown here as an average between samples of the same sample site shown in Figure 3. Color indicates PMA index value. Saturation indicates confidence (sigma) in the PMA index value and was calculated using the standard deviation of PMA index across the samples that went into that pixel. Bacterial taxa are ordered by decreasing overall relative abundance. Each square represents the average of at least four samples taken from different individuals. PMA-index is calculated by comparing the relative abundance of a given taxon as measured by PMA-seq (A_{PMA}) to the sum of the relative abundance for that taxon in both traditional sequencing (A_{trad}) and PMA-seq. (B) Relative abundance at each body site for the top three most abundant (overall) bacterial taxa as assessed by traditional sequencing and PMA-seq. Colors of bars correspond to colors in Figure 2F. *Relative abundance data for Staphylococcaceae was determined using forward-read sequencing information only.

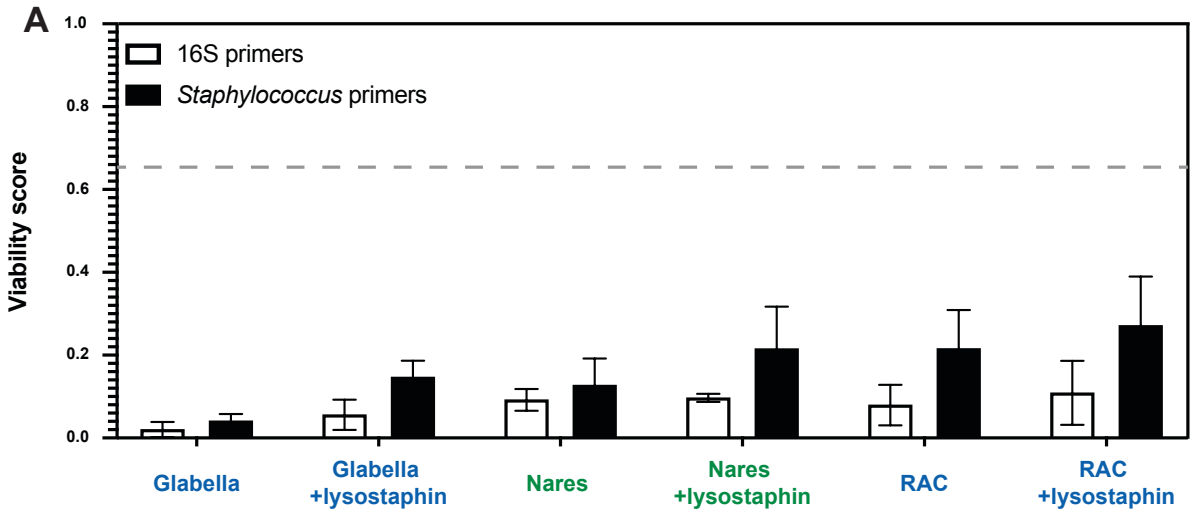

Figure 4 – figure supplement 1: Viability score for three skin sites using lysostaphin and *Staphylococcus*-specific PCR primers. (A)The three skin sites with the most abundant bacterial DNA are shown. Half of each sample was treated with lysostaphin prior to DNA isolation to assess how the viability score would change. ddPCR was performed on each sample using both 16S primers (white bars) and *Staphylococcus*-specific (black bars) primers. The dashed line indicates the average viability score of non-skin microbiome sites (0.66). N=3 for all.

413
414 **The spatial organization and viability of mouse skin microbiome is similar to that of**
415 **humans**

416 While our human skin microbiome FISH and PMA studies strongly agree, we are unable
417 to directly compare the two approaches on the same samples. For a system in which we could
418 perform both FISH and PMA-ddPCR on the same samples we turned to mouse skin, which also
419 enabled us to ask if our findings are human-specific. We assessed the spatial distribution of
420 bacterial cells in mouse skin tissue using the universal bacterial EUB338 FISH probe with tissue
421 from K14-H2B-GFP mice. We observed the same bacterial distributions as seen in the human
422 tissues: a high abundance of bacteria in hair follicles (enrichment score of 15.26) with relatively
423 few bacteria on the skin surface (enrichment score of 0.21) (Figure 5A, D). To test how fur
424 impacts the presence of bacteria on the skin surface, we performed FISH staining on skin from
425 nude mice (SKH1-Hrhr Elite) and found similar bacterial distributions (follicle-associated
426 enrichment score of 10.79 compared to 1.13 for the skin surface) (Figure 5B, D). The significant
427 numbers of bacteria observed in hair follicles suggests that the absence of surface bacteria is not
428 merely due to the relatively clean conditions in which laboratory mice are housed. Because the
429 mouse tissue was untreated with any sterilizing agents prior to dissection, these results also
430 suggest that the low numbers of skin-surface-associated bacteria found in the human tissue
431 samples are not simply a result of pre-biopsy sterilization.

432 Since we did not detect many bacteria on the surface of any of the skin samples tested,
433 we sought a positive control to confirm that our FISH staining can visualize bacteria on the skin
434 surface if they are present. For example, it is possible that the dry, acidic nature of the skin
435 affects FISH efficacy, leading to little staining at the skin surface. To this end, we applied *E. coli*
436 cells to dorsal mouse skin tissue after removing it from the animal. This tissue was then

437 processed in the same way as the human and other mouse tissue. FISH staining revealed many
438 bacteria on the surface of these samples, confirming that this technique can be used to reliably
439 visualize bacteria on the skin surface (Figure 5C). As a negative control, we also confirmed that
440 a probe encoding the reverse complement of the EUB338 FISH probe (NONEUB338) did not
441 significantly hybridize to the skin surface or follicles (Figure 5C). These results support the
442 conclusions from our FISH experiments on human tissues by demonstrating EUB338 staining
443 works well in the biological context of the skin surface.

444 We next assessed the viability of bacteria in the mouse skin microbiome using PMA-
445 ddPCR. As further evidence that our previous findings are not human-specific, the PMA-ddPCR-
446 based viability score for mouse skin microbiome sites was similar to the average viability score
447 for human skin sites (0.066 and 0.045 respectively) and was much lower than the viability score
448 for the mouse or human fecal microbiome (0.98 and 0.66 respectively). (Figure 5E). These
449 results indicate that, despite having distinct skin biology, both humans and mice have an
450 abundance of bacterial DNA on the skin surface that is not associated with viable cells.

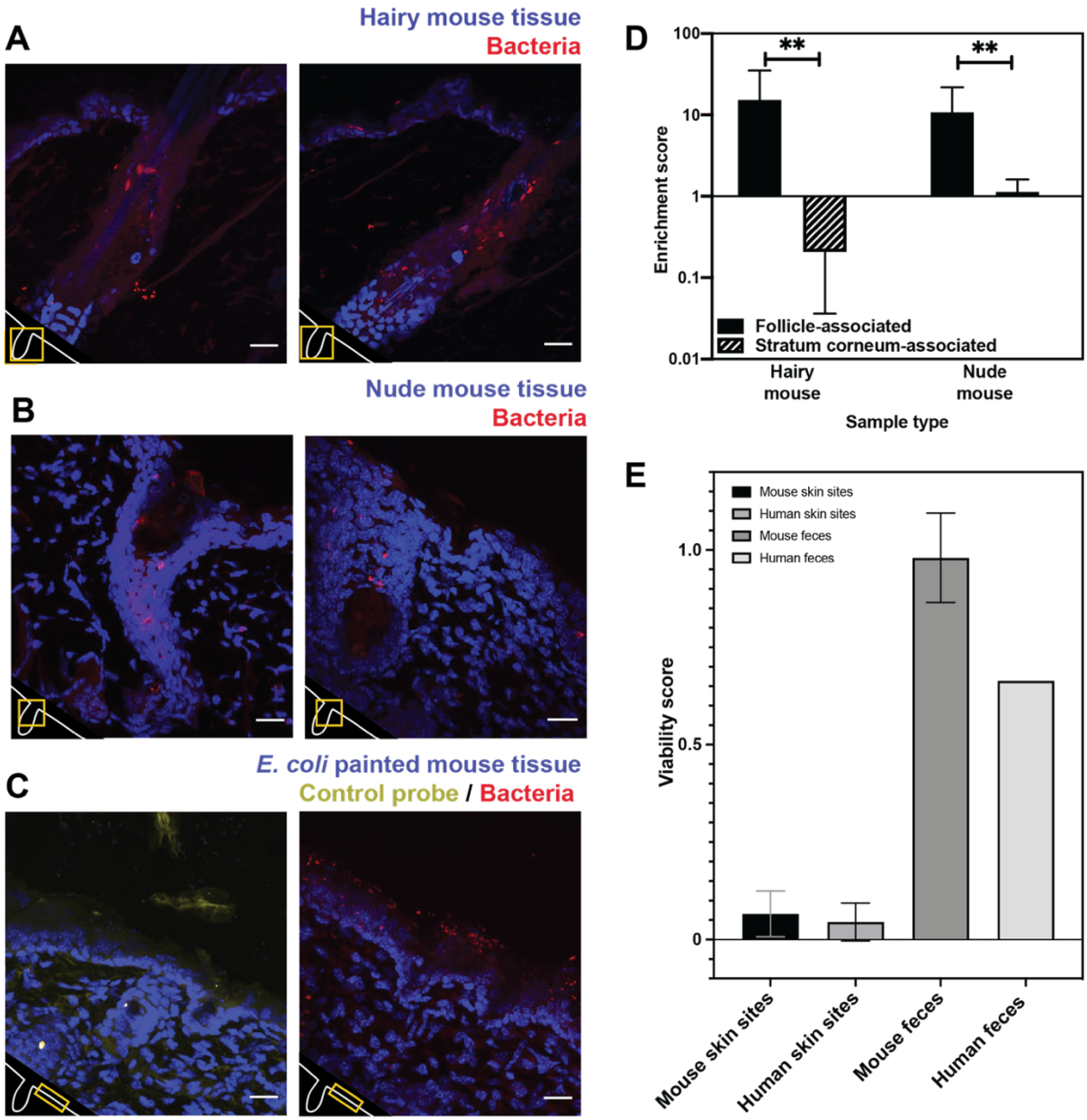

Figure 5: Bacterial FISH staining of mouse tissue (A-D) and comparison of mouse viability scores and human viability scores. (A). Tissues from a K14-H2B_GFP mouse stained with EUB338 show abundant bacterial signal in hair follicles but not on the skin surface. (B) Tissues from SKH1-Hrhr Elite nude mice also show bacterial presence concentrated to cutaneous structures and not at the skin surface. (C) E. coli applied to C57BL/6 mouse tissue was stained with either EUB338 (in red) or its complementary strand control probe NONEUB338 (in yellow). (D) Quantification enrichment scores showing the median and interquartile range. Significance was calculated using the Mann-Whitney test. *P ≤ 0.05, **P ≤ 0.01, N = 6 for hairy mouse follicle, nude mouse follicle, and hairy mouse stratum corneum, N = 5 nude mouse stratum corneum. (E) The PMA-ddPCR-based viability scores for mouse skin microbiomes are much lower than for mouse fecal microbiomes (0.66 and 0.98 respectively). These viability scores for mouse sites are very similar to those for humans (0.066 and 0.045 for skin microbiomes, 0.98 and 0.66 for fecal microbiomes).

465 **Skin surface repopulation is driven by stable communities of bacteria below the skin**
466 **surface**

467 Finally, we sought to determine the functional significance of our findings in the context
468 of skin microbiome surface perturbation and repopulation. Specifically, we performed a
469 perturbation-recovery experiment in which the skin microbiome of the forehead from healthy
470 volunteers was sampled at time T=0 to establish a baseline microbial community, sterilized with
471 benzalkonium chloride, and then sampled 3, 24, and 48 hours later to monitor recovery (Figure
472 6A). At each sampling timepoint, half of the sample was treated with PMA prior to DNA
473 isolation and subsequent 16S rRNA gene sequencing. Focusing on the PMA-untreated samples,
474 we found that 4 of the 5 volunteers demonstrated significant reduction in the absolute amount of
475 DNA upon sterilization (Figure 6B), but that the overall bacterial composition of the skin
476 microbiome remained relatively stable (Figure 6A, all bacteria listed in Figure 6 – figure
477 supplement 2.). It should be noted that, although the skin microbiome composition found in
478 volunteer 4 is markedly different than the communities identified in the other volunteers, the
479 species identified are still common constituents of a healthy skin microbiome. Additionally,
480 volunteer 4 had a lower abundance of bacterial DNA overall, which might lead to the lower
481 relative abundance of *Propionibacteriaceae.*

482 Our findings recapitulate the previously-reported paradox that the skin microbiome is
483 both unstable at short timescales and stable at long timescales (*11*, *23*). Importantly, analysis of
484 the PMA-treated samples enabled us to understand the recovery dynamics. Specifically, we used
485 Bray-Curtis dissimilarity to monitor the extent of population recovery (Figure 6C). We found
486 that comparing samples with and without the use of PMA to the PMA-treated baseline
487 community resulted in a consistent pattern across all individuals. Over the course of the

488 experiment, the communities converged back to the PMA-treated baseline samples but showed
489 no consistent patterns of similarity relative to the PMA-untreated baseline samples (Figure 6 –
490 figure supplement 2A). This result supports the hypothesis that bacterial DNA on the skin
491 surface can be readily removed and is continuously replenished by viable bacterial populations in
492 protected reservoirs below the skin surface.

493 Examining repopulation dynamics more finely at the ASV level revealed that ASVs that
494 were lost upon surface sterilization often re-appeared over time, consistent with the model that
495 surface repopulation can be driven by subsurface populations. Specifically, we found that after
496 surface sterilization, the skin is repopulated by the same ASVs as were present before
497 sterilization (Figure 6 – figure supplement 2B). In Figure 6 – figure supplement 2B we highlight
498 specific examples in which a given ASV appears in the live-cell population (+PMA) prior to
499 surface sterilization (T0), disappears from the live-cell population following sterilization (T3),
500 and later re-appears in the live-cell population either 24 or 48 hours later. Together, these results
501 suggest that bacteria thrive in protected areas below the skin surface and that the DNA of their
502 dead remains accumulates on the skin surface. In this way, the bacterial DNA on the skin surface
503 acts as a fingerprint of the communities below.
504

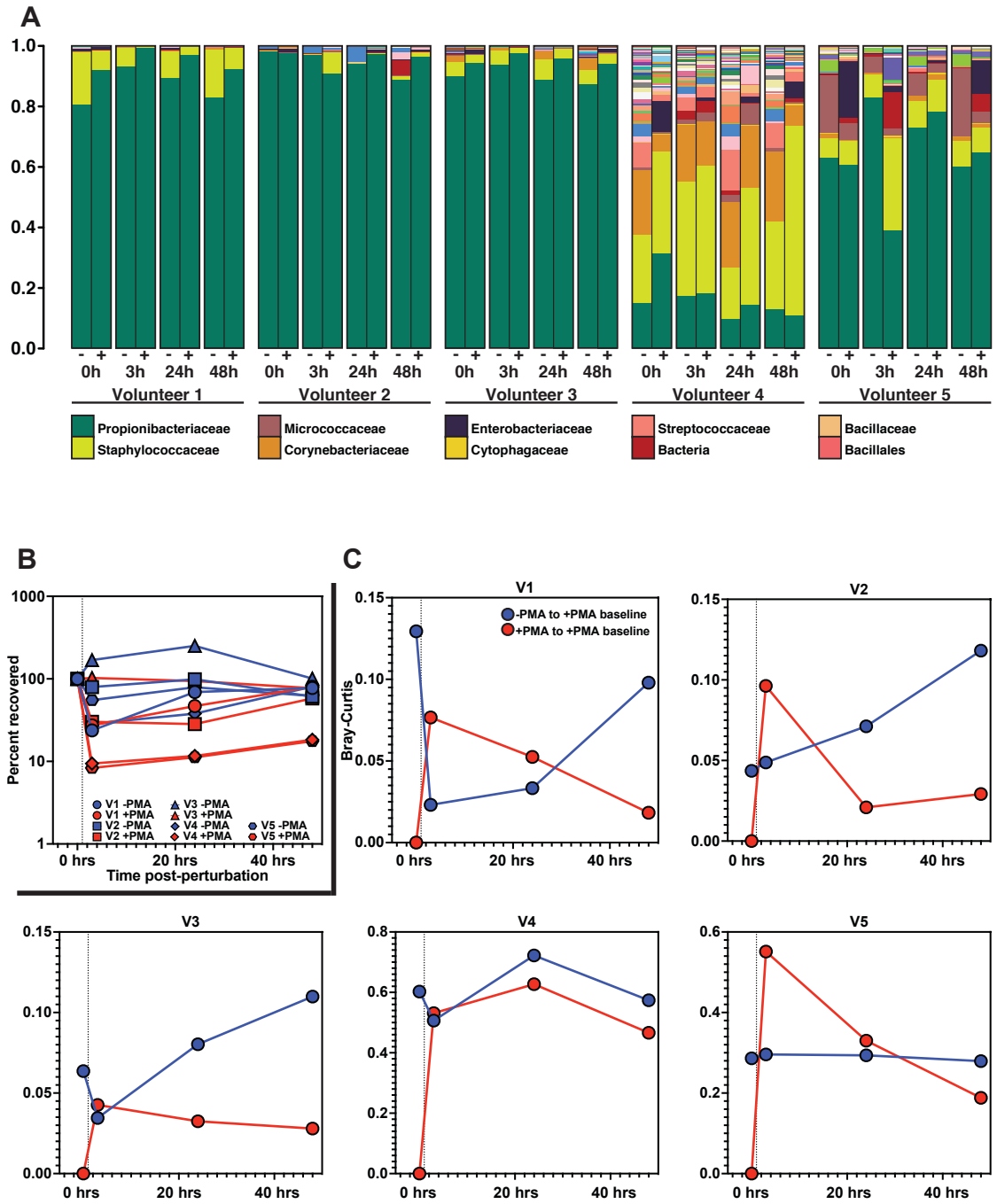

Figure 6: Skin microbiome perturbation and recovery. (A) Bacterial relative abundance in each individual over the 48 hours following perturbation. 0 hour represents baseline, pre-perturbation community. Whether a sample was treated with PMA is indicated by (-) and (+). (B) Quantification of bacterial DNA recovery over the 48 hours following perturbation. DNA was quantified using ddPCR. (C) Bray-Curtis dissimilarity of each individual over the 48 hours following perturbation. Red data points are comparing PMA-treated samples to the PMA-treated baseline sample. Blue data points are comparing PMA-untreated samples to the PMA-treated baseline sample. Dashed vertical line indicates the point of perturbation.

k__Bacteria.p__Actinobacteria.c__Actinobacteria.o__Actinomycetales.f__Propionibacteriaceae
k__Bacteria.p__Firmicutes.c__Bacilli.o__Bacillales.f__Staphylococcaceae
k__Bacteria.p__Actinobacteria.c__Actinobacteria.o__Actinomycetales.f__Corynebacteriaceae
k__Bacteria.p__Bacteroidetes.c__Cytophagia.o__Cytophagales.f__Cytophagaceae
k__Bacteria.p__Actinobacteria.c__Actinobacteria.o__Actinomycetales.f__Micrococcaceae
k__Bacteria.__.__.__.__
k__Bacteria.p__Proteobacteria.c__Gammaproteobacteria.o__Enterobacteriales.f__Enterobacteriaceae
k__Bacteria.p__Firmicutes.c__Bacilli.o__Lactobacillales.f__Streptococcaceae
k__Bacteria.p__Firmicutes.c__Bacilli.o__Bacillales.f__Bacillaceae
k__Bacteria.p__Firmicutes.c__Bacilli.o__Bacillales.__
k__Bacteria.p__Firmicutes.c__Clostridia.o__Clostridiales.f__.Tissierellaceae.
k__Bacteria.p__Proteobacteria.c__Betaproteobacteria.o__Neisseriales.f__Neisseriaceae
k__Bacteria.p__Proteobacteria.c__Betaproteobacteria.o__Burkholderiales.f__Comamonadaceae
k__Bacteria.p__Proteobacteria.c__Alphaproteobacteria.o__Rickettsiales.f__
k__Bacteria.p__Proteobacteria.c__Betaproteobacteria.o__Burkholderiales.f__Oxalobacteraceae
k__Bacteria.p__Actinobacteria.c__Actinobacteria.o__Actinomycetales.f__Brevibacteriaceae
k__Bacteria.p__Bacteroidetes.c__Flavobacteriia.o__Flavobacteriales.f__.Weeksellaceae.
k__Bacteria.p__Proteobacteria.c__Gammaproteobacteria.o__Xanthomonadales.f__Xanthomonadaceae
k__Bacteria.p__Firmicutes.c__Bacilli.o__Gemellales.f__Gemellaceae
k__Bacteria.p__Proteobacteria.c__Alphaproteobacteria.o__Rhizobiales.f__Methylobacteriaceae
k__Bacteria.p__Proteobacteria.c__Alphaproteobacteria.o__Sphingomonadales.f__Sphingomonadaceae
k__Bacteria.p__Firmicutes.c__Bacilli.o__Lactobacillales.f__Leuconostocaceae
k__Bacteria.p__Proteobacteria.c__Alphaproteobacteria.o__Rhodobacterales.f__Rhodobacteraceae
k__Bacteria.p__Actinobacteria.c__Actinobacteria.o__Actinomycetales.f__Microbacteriaceae
k__Bacteria.p__Cyanobacteria.c__Chloroplast.o__Streptophyta.f__
k__Bacteria.p__Bacteroidetes.c__.Saprospirae..o__.Saprospirales..f__Chitinophagaceae
k__Bacteria.p__Cyanobacteria.c__Synechococcophycideae.o__Pseudanabaenales.f__Pseudanabaenaceae
k__Bacteria.p__Fusobacteria.c__Fusobacteriia.o__Fusobacteriales.f__Fusobacteriaceae
k__Bacteria.p__Bacteroidetes.c__Bacteroidia.o__Bacteroidales.f__.Paraprevotellaceae.
k__Bacteria.p__Firmicutes.c__Bacilli.o__Lactobacillales.f__Aerococcaceae
k__Bacteria.p__Firmicutes.c__Bacilli.o__Lactobacillales.f__Carnobacteriaceae
k__Bacteria.p__Bacteroidetes.c__Bacteroidia.o__Bacteroidales.f__Porphyromonadaceae
k__Bacteria.p__Bacteroidetes.c__Flavobacteriia.o__Flavobacteriales.f__Flavobacteriaceae
k__Bacteria.p__Firmicutes.c__Clostridia.o__Clostridiales.f__Ruminococcaceae
k__Bacteria.p__Proteobacteria.c__Gammaproteobacteria.o__Pseudomonadales.f__Moraxellaceae
k__Bacteria.p__Proteobacteria.c__Alphaproteobacteria.o__Caulobacterales.f__Caulobacteraceae
k__Bacteria.p__Proteobacteria.c__Betaproteobacteria.o__Burkholderiales.f__Burkholderiaceae
k__Bacteria.p__Firmicutes.c__Clostridia.o__Clostridiales.f__Veillonellaceae
k__Bacteria.p__Actinobacteria.c__Actinobacteria.o__Actinomycetales.f__Intrasporangiaceae
k__Bacteria.p__Fusobacteria.c__Fusobacteriia.o__Fusobacteriales.f__Leptotrichiaceae
k__Bacteria.p__Bacteroidetes.c__Bacteroidia.o__Bacteroidales.f__Prevotellaceae
k__Bacteria.p__Firmicutes.c__Clostridia.o__Clostridiales.f__Clostridiaceae
k__Bacteria.p__Actinobacteria.c__Actinobacteria.o__Actinomycetales.f__Dermabacteraceae
k__Bacteria.p__Cyanobacteria.c__Chloroplast.o__Stramenopiles.f__
k__Bacteria.p__Proteobacteria.c__Alphaproteobacteria.o__.f__
k__Bacteria.p__Proteobacteria.c__Gammaproteobacteria.o__Pseudomonadales.f__Pseudomonadaceae
k__Bacteria.p__Actinobacteria.c__Actinobacteria.o__Actinomycetales.__
k__Bacteria.p__.Thermi..c__Deinococci.o__Deinococcales.f__Deinococcaceae
k__Bacteria.p__Proteobacteria.c__Alphaproteobacteria.o__Rhizobiales.f__Rhizobiaceae
k__Bacteria.p__Proteobacteria.c__Deltaproteobacteria.o__FAC87.f__
k__Bacteria.p__Bacteroidetes.c__Bacteroidia.o__Bacteroidales.f__Bacteroidaceae
k__Bacteria.p__Cyanobacteria.c__Synechococcophycideae.o__Synechococcales.f__Acaryochloridaceae
k__Bacteria.p__Firmicutes.c__Bacilli.o__Lactobacillales.f__Enterococcaceae
k__Bacteria.p__Proteobacteria.__.__.__
k__Bacteria.p__Actinobacteria.c__Actinobacteria.o__Actinomycetales.f__Mycobacteriaceae
k__Bacteria.p__Proteobacteria.c__Alphaproteobacteria.o__Rhodospirillales.f__Acetobacteraceae
k__Bacteria.p__Proteobacteria.c__Alphaproteobacteria.o__Rhizobiales.f__Bradyrhizobiaceae
k__Bacteria.p__Actinobacteria.c__Actinobacteria.o__Actinomycetales.f__Gordoniaceae
k__Bacteria.p__Proteobacteria.c__Gammaproteobacteria.o__Legionellales.f__Legionellaceae
k__Bacteria.p__Firmicutes.c__Erysipelotrichi.o__Erysipelotrichales.f__Erysipelotrichaceae
k__Bacteria.p__Bacteroidetes.c__Sphingobacteriia.o__Sphingobacteriales.f__Sphingobacteriaceae
k__Bacteria.p__Actinobacteria.c__Actinobacteria.o__Actinomycetales.f__Actinomycetaceae
k__Bacteria.p__Proteobacteria.c__Alphaproteobacteria.o__Rickettsiales.f__mitochondria
k__Bacteria.p__TM7.c__TM7.3.o__.f__
k__Bacteria.p__Firmicutes.c__Bacilli.o__Lactobacillales.f__Lactobacillaceae
k__Bacteria.p__Firmicutes.c__Clostridia.o__Clostridiales.f__Lachnospiraceae
k__Bacteria.p__Actinobacteria.c__Actinobacteria.o__Actinomycetales.f__Williamsiaceae
k__Bacteria.p__Proteobacteria.c__Alphaproteobacteria.o__Rhizobiales.f__Aurantimonadaceae
k__Bacteria.p__Firmicutes.c__Clostridia.o__Clostridiales.f__
k__Bacteria.p__Proteobacteria.c__Alphaproteobacteria.o__Rhizobiales.f__
k__Bacteria.p__Proteobacteria.c__Alphaproteobacteria.o__Rhizobiales.f__Hyphomicrobiaceae
k__Bacteria.p__Firmicutes.c__Clostridia.o__Clostridiales.__
k__Bacteria.p__Proteobacteria.c__Epsilonproteobacteria.o__Campylobacterales.f__Campylobacteraceae
k__Bacteria.p__Proteobacteria.c__Gammaproteobacteria.o__Pasteurellales.f__Pasteurellaceae
k__Bacteria.p__Proteobacteria.c__Alphaproteobacteria.o__Rhizobiales.f__Beijerinckiaceae
k__Bacteria.p__Proteobacteria.c__Betaproteobacteria.o__Rhodocyclales.f__Rhodocyclaceae
k__Bacteria.p__SR1.c__.o__.f__
k__Bacteria.p__Proteobacteria.c__Gammaproteobacteria.o__Xanthomonadales.f__Sinobacteraceae
k__Bacteria.p__Actinobacteria.c__Actinobacteria.o__Actinomycetales.f__Nocardioidaceae
k__Bacteria.p__Acidobacteria.c__.Chloracidobacteria..o__RB41.f__
k__Bacteria.p__Actinobacteria.c__Acidimicrobiia.o__Acidimicrobiales.f__
k__Bacteria.p__Proteobacteria.c__Deltaproteobacteria.o__Myxococcales.f__
k__Bacteria.p__Firmicutes.c__Clostridia.o__Clostridiales.f__Peptostreptococcaceae
k__Bacteria.p__Proteobacteria.c__Alphaproteobacteria.o__Rhizobiales.f__Brucellaceae
k__Bacteria.p__Proteobacteria.c__Alphaproteobacteria.o__Rhizobiales.f__Xanthobacteraceae
k__Bacteria.p__Firmicutes.c__Clostridia.o__OPB54.f__
k__Bacteria.p__Actinobacteria.c__Thermoleophilia.o__Solirubrobacterales.f__Patulibacteraceae
k__Bacteria.p__Proteobacteria.c__Gammaproteobacteria.o__Vibrionales.f__Pseudoalteromonadaceae
k__Bacteria.p__Proteobacteria.c__Alphaproteobacteria.o__Rhizobiales.f__Methylocystaceae
k__Bacteria.p__Firmicutes.c__Clostridia.o__Clostridiales.f__.Mogibacteriaceae.
k__Bacteria.p__Firmicutes.c__Bacilli.o__Lactobacillales.f__
k__Bacteria.p__Actinobacteria.c__Actinobacteria.o__Actinomycetales.f__Dietziaceae
k__Bacteria.p__Proteobacteria.c__Alphaproteobacteria.o__BD7.3.f__
k__Bacteria.p__Firmicutes.c__Bacilli.o__Bacillales.f__Paenibacillaceae
k__Bacteria.p__Acidobacteria.c__.Chloracidobacteria..o__PK29.f__
k__Bacteria.p__Actinobacteria.c__Actinobacteria.o__Actinomycetales.f__
k__Bacteria.p__Chlorobi.c__OPB56.o__.f__
k__Bacteria.p__Actinobacteria.c__Coriobacteriia.o__Coriobacteriales.f__Coriobacteriaceae
k__Bacteria.p__Proteobacteria.c__Alphaproteobacteria.o__Rhodospirillales.f__Rhodospirillaceae
Unassigned.__.__.__.__
k__Bacteria.p__Acidobacteria.c__.Chloracidobacteria..o__RB41.f__Ellin6075
k__Bacteria.p__Firmicutes.c__Bacilli.o__Bacillales.f__.Exiguobacteraceae.
k__Bacteria.p__TM7.c__TM7.3.o__CW040.f__
k__Bacteria.p__Firmicutes.c__Clostridia.o__Clostridiales.f__.Acidaminobacteraceae.
k__Bacteria.p__Planctomycetes.c__Planctomycetia.o__Gemmatales.f__Gemmataceae
k__Bacteria.p__Proteobacteria.c__Deltaproteobacteria.o__MIZ46.f__
k__Bacteria.p__Spirochaetes.c__.Leptospirae..o__.Leptospirales..f__Leptospiraceae
k__Bacteria.p__TM7.c__TM7.3.o__EW055.f__
k__Bacteria.p__Firmicutes.c__Bacilli.o__Bacillales.f__Listeriaceae
k__Bacteria.p__Verrucomicrobia.c__.Pedosphaerae..o__.Pedosphaerales..f__
k__Bacteria.p__Firmicutes.c__Bacilli.o__Bacillales.f__Planococcaceae
k__Bacteria.p__Actinobacteria.c__Actinobacteria.o__Actinomycetales.f__Nocardiaceae
k__Bacteria.p__Firmicutes.c__Bacilli.o__Bacillales.f__Thermoactinomycetaceae
k__Bacteria.p__GN02.c__BD1.5.o__.f__
k__Bacteria.p__.c__.o__.f__
k__Bacteria.p__Actinobacteria.c__Actinobacteria.o__Actinomycetales.f__Cellulomonadaceae
k__Bacteria.p__Tenericutes.c__Mollicutes.o__RF39.f__
k__Bacteria.p__Proteobacteria.c__Betaproteobacteria.o__Burkholderiales.f__Alcaligenaceae
k__Bacteria.p__Firmicutes.c__Bacilli.o__Gemellales.f__
k__Bacteria.p__Cyanobacteria.c__Oscillatoriophycideae.o__Chroococcales.f__Xenococcaceae
k__Bacteria.p__Actinobacteria.c__Thermoleophilia.o__Solirubrobacterales.f__
k__Bacteria.p__Actinobacteria.c__Actinobacteria.o__Actinomycetales.f__Sporichthyaceae
k__Bacteria.p__Proteobacteria.c__Gammaproteobacteria.o__Alteromonadales.f__.Chromatiaceae.
k__Bacteria.p__Chloroflexi.c__Chloroflexi.o__.Roseiflexales..f__.Kouleothrixaceae.
k__Bacteria.p__Proteobacteria.c__Alphaproteobacteria.o__Rhodospirillales.f__
k__Bacteria.p__Proteobacteria.c__Alphaproteobacteria.o__Rhizobiales.f__Phyllobacteriaceae
k__Bacteria.p__Cyanobacteria.__.__.__
k__Bacteria.p__Chloroflexi.c__Anaerolineae.o__A31.f__S47
k__Bacteria.p__Chloroflexi.c__Anaerolineae.o__Anaerolineales.f__Anaerolinaceae
k__Bacteria.p__.Thermi..c__Deinococci.o__Thermales.f__Thermaceae
k__Bacteria.p__TM7.c__TM7.3.__.__
k__Bacteria.p__Proteobacteria.c__Deltaproteobacteria.o__Sva0853.f__JTB36
k__Bacteria.p__Firmicutes.c__Clostridia.o__Clostridiales.f__Peptococcaceae
k__Bacteria.p__Actinobacteria.c__Actinobacteria.o__Actinomycetales.f__Pseudonocardiaceae
k__Bacteria.p__Proteobacteria.c__Epsilonproteobacteria.o__Campylobacterales.f__Helicobacteraceae
k__Bacteria.p__FBP.c__.o__.f__
k__Bacteria.p__Tenericutes.c__RF3.o__ML615J.28.f__
k__Bacteria.p__Planctomycetes.c__Planctomycetia.o__Gemmatales.f__Isosphaeraceae
k__Bacteria.p__Proteobacteria.c__Epsilonproteobacteria.o__Campylobacterales.f__
k__Bacteria.p__Cyanobacteria.c__4C0d.2.o__MLE1.12.f__
k__Bacteria.p__Proteobacteria.c__Alphaproteobacteria.o__Rhizobiales.__
k__Bacteria.p__Cyanobacteria.c__Chloroplast.o__Chlorophyta.f__Trebouxiophyceae
k__Bacteria.p__Proteobacteria.c__Betaproteobacteria.o__Methylophilales.f__Methylophilaceae
k__Bacteria.p__Actinobacteria.c__Actinobacteria.o__Actinomycetales.f__Beutenbergiaceae
k__Bacteria.p__Planctomycetes.c__Phycisphaerae.o__WD2101.f__
k__Bacteria.p__Proteobacteria.c__Gammaproteobacteria.o__Cardiobacteriales.f__Cardiobacteriaceae
k__Bacteria.p__Proteobacteria.c__Deltaproteobacteria.o__Myxococcales.f__Myxococcaceae
k__Bacteria.p__Bacteroidetes.c__Sphingobacteriia.o__Sphingobacteriales.f__
k__Bacteria.p__Spirochaetes.c__Spirochaetes.o__Spirochaetales.f__Spirochaetaceae
k__Bacteria.p__Tenericutes.c__Mollicutes.o__Acholeplasmatales.f__Acholeplasmataceae
k__Bacteria.p__Proteobacteria.c__Betaproteobacteria.o__Burkholderiales.f__
k__Bacteria.p__Tenericutes.c__Mollicutes.o__Mycoplasmatales.f__Mycoplasmataceae
k__Bacteria.p__Proteobacteria.c__Betaproteobacteria.__.__
k__Bacteria.p__Actinobacteria.c__Thermoleophilia.o__Solirubrobacterales.f__Solirubrobacteraceae
k__Bacteria.p__TM7.c__TM7.1.o__.f__
k__Bacteria.p__Synergistetes.c__Synergistia.o__Synergistales.f__Dethiosulfovibrionaceae
k__Bacteria.p__Bacteroidetes.c__Bacteroidia.o__Bacteroidales.f__

Figure 6 – figure supplement 1: List of bacteria identified in perturbation recovery. The bacterial groups listed here correspond to the entire sequencing dataset shown in Figure 6. Bacteria are listed in order of relative abundance.

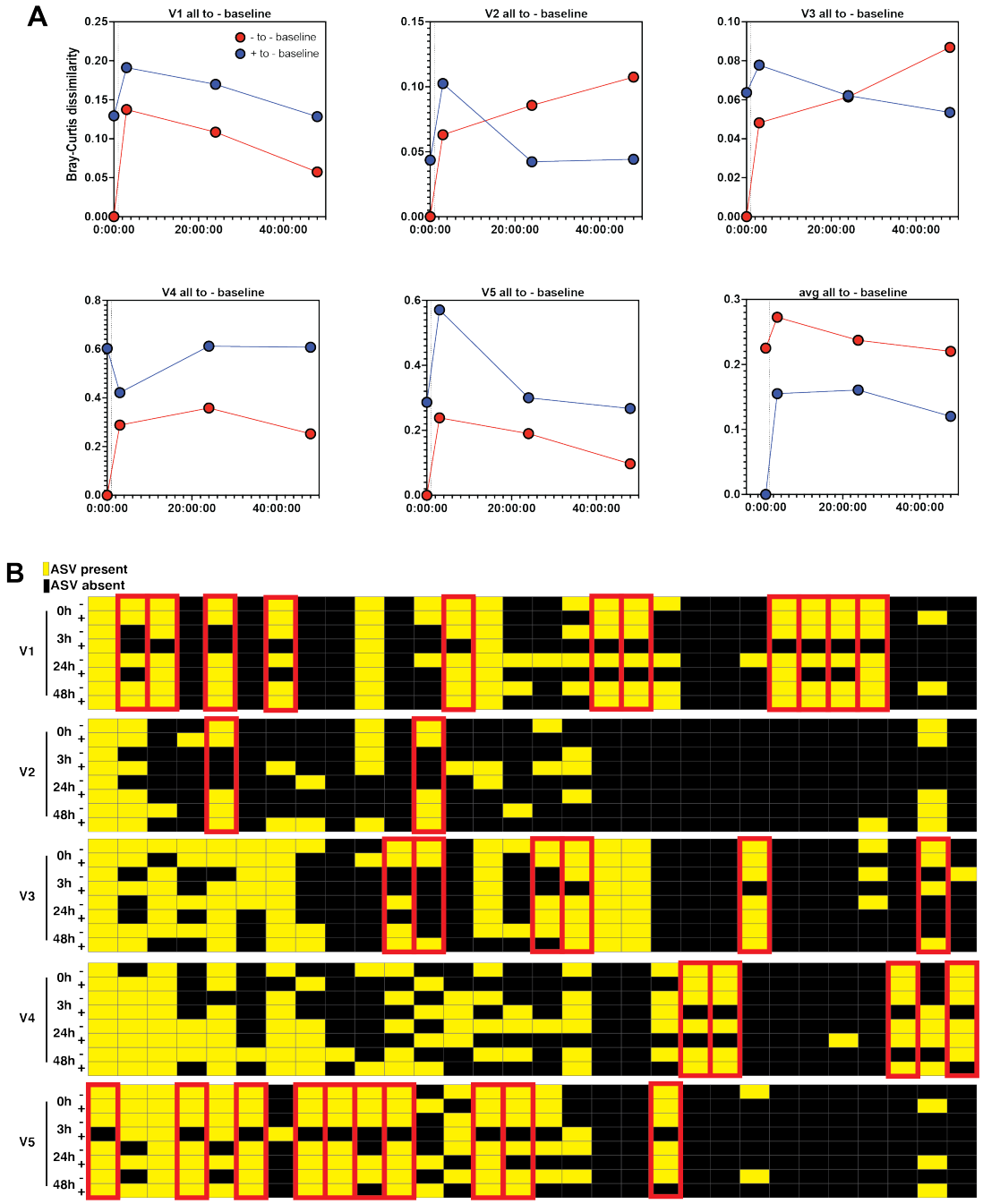

Figure 6 – figure supplement 2: Skin microbiome perturbation and recovery. (A) Bray-Curtis dissimilarity of each individual over the 48 hours following perturbation. Red data points are comparing PMA-treated samples to the PMA-untreated baseline sample. Blue data points are comparing PMA-untreated samples to the PMA-untreated baseline sample. Dashed vertical line indicates the point of perturbation. (B) ASV-level relative abundance converted into binary dataset in which each ASV present at greater than 1% appears in yellow and each absent ASV appears in black. Columns are ASVs and rows are PMA-treated or PMA-untreated perturbation recovery samples. ASVs indicated in red follow a specific pattern of repopulation in which the ASV is present in the live cells (+PMA) at T=0, disappears from the live cells after perturbation (T=3), and then recovers in the live population at either T=24 or T=48.

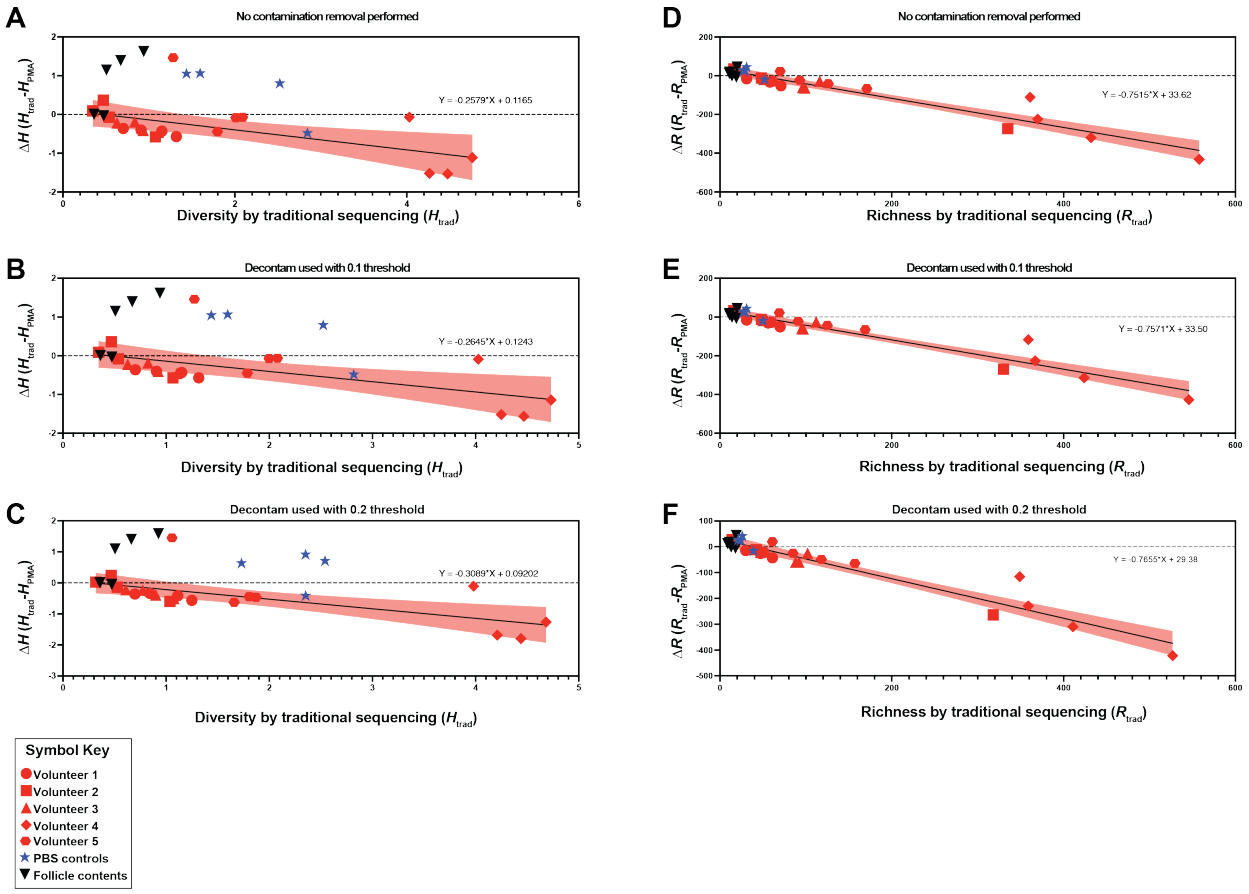

Figure 6 – figure supplement 3. Contamination removal performed on 600nt sequencing data. The Shannon diversity changes between traditional sequencing (H_{trad}) and PMA-seq (H_{PMA}) are demonstrated by plotting the change in diversity (ΔH) against H_{trad} (A-C). The richness changes between traditional sequencing (R_{trad}) and PMA-seq (R_{PMA}) are demonstrated by plotting the change in richness (ΔR) against R_{trad} (D-F). Analysis with no decontamination removal (A, D), decontamination removal using the Decontam program in R with a 0.1 threshold (B, E), and decontamination removal using the Decontam program in R with a 0.2 threshold (C, F) are all shown. Symbols in red represent samples associated with the perturbation recovery data (Figure 6). Symbols in blue represent PBS DNA isolation controls. Symbols in black represent follicle contents obtained from single follicles. The shaded red region represents the 95% confidence interval for the linear regression performed using only the perturbation recovery samples (red symbols).

544 **Discussion**

545 Here we used both imaging and PMA-based methods to demonstrate that the skin surface is
546 sparsely colonized by bacteria. This central finding holds true across skin from human biopsies,
547 healthy swabbed volunteers, hairy mice, and nude mice. The skin microbiome has garnered a
548 great deal of attention as a means for educating the immune system, combatting pathogens, and
549 promoting wound healing, and multiple groups are pursuing skin probiotics (*24*). Our findings
550 have significant implications for the mechanisms underlying these skin microbiome functions, as
551 well as for the ability to manipulate skin microbiome composition. For example, our findings
552 support previous work suggesting that the key function of immune education by the skin
553 microbiome occurs within hair follicles (*4*), though cell-free DNA on the skin surface could also
554 impact the immune system. Our findings also support previous work showing that individual
555 pores are colonized by clonal bacterial populations (*25*). Meanwhile, our results may help to
556 explain why stably colonizing the skin surface with exogenous bacteria has proved to be difficult
557 and often requires abrasion (*3*). Disruption of the stratum corneum (skin surface layers), which
558 occurs during skin abrasion, may allow access to the deeper layers of tissue where the stable
559 bacterial populations reside. Thus, targeting the bacteria within hair follicles may represent a
560 better strategy for stably manipulating the skin microbiome or educating the immune system.
561 While it has been known for some time that bacteria inhabit hair follicles (*4*, *15*), our findings
562 extend this knowledge and suggest that the viable bacteria of the skin microbiome are primarily
563 restricted to these sites. This is further supported by our finding that bacteria can be readily
564 cultured from the skin surface, but at far less abundance than suggested by the amount of
565 bacterial DNA present on the skin.

566 Our results also offer insight into the apparent paradox of skin microbiome stability, in
567 which skin microbiome composition has been found to be both stable over long time scales and
568 susceptible to transient perturbations (*11*, *23*). The skin is primarily colonized by viable bacteria
569 in pilosebaceous units and other skin invaginations and the bacterial DNA on the skin surface is
570 mostly from dead bacteria. We show that surface bacterial DNA could be easily washed away,
571 while the viable subsurface bacteria remain unperturbed by washing, persisting as a small but
572 stable source of new bacterial DNA that replenishes the skin surface over time. This model also
573 explains the counter-intuitive abundance of obligately anaerobic bacterial species associated with
574 the skin microbiome. Human skin cells are also born below the skin surface and are pushed to
575 the surface as they die. In this way, the life cycle of the skin microbiome may resemble the
576 process of epithelial cell turnover in the skin.

577 Our findings also raise fundamental questions that will need to be addressed by future
578 studies focused on why the skin surface is poorly colonized. The accessible DNA in non-skin
579 microbiomes is generally representative of viable bacterial cells, as all non-skin microbiomes
580 tested had viability scores above 0.4. This is in stark contrast to the skin microbiome, which had
581 viability scores between 0.02 and 0.12. Even saliva, which contains many antimicrobial
582 compounds (*26*), had a viability score nearly four times greater than the highest viability score
583 for a skin microbiome. The uniquely low viability score associated with the skin could be
584 explained by passive mechanisms, like bacterial DNA adhering to the skin long after a bacterial
585 cell dies. Alternatively, there could be active mechanisms like bacterial killing on the skin
586 surface by factors like antimicrobial peptides produced by epithelial cells, competition between
587 bacterial species, or exposure to harsh environmental factors such as starvation, UV radiation, or

588 desiccation. Another open question is whether similar trends hold true for non-bacterial

589 components of the skin microbiome like fungi and viruses.

590 **Materials and Methods**

591 **Human and mouse tissue processing**

592 Human tissue was obtained through the Skin Translational Research Core within the Skin
593 Biology and Diseases Resource-based Center (SBDRC) at the University of Pennsylvania.
594 Normal adult human skin was obtained during skin cancer surgery procedures. After the
595 cancerous tissue is removed, normal (non-cancerous) tissue must also be removed to ensure a
596 cosmetic repair. These tissue portions are normally discarded, but were collected for imaging.
597 Surgical scrub solution was used prior to the procedure (alcohol/iodine or chlorhexidine).
598 Tissues were embedded in room temperature OCT immediately upon excision and stored at -
599 80°C. Tissues were obtained from the forehead of a 32-year-old female and the cheek of an 81-
600 year-old male. Tissues were obtained through the Core B- Skin Translational Research Core at
601 the SBDRC as part of the "Fresh normal and diseased human skin" service.

602 All mice were housed and maintained in a certified animal facility and all experiments
603 were conducted according to USA Public Health Service Policy of Humane Care and Use of
604 Laboratory Animals. All protocols were approved by the Institutional Animal Care and Use
605 Committee, protocol #1867-17 (Princeton University). Dorsal skin from K14-H2B-GFP,
606 C57BL/6, and SKH1-Elite nude mice was used for fluorescence experiments. The fur from K14-
607 H2B-GFP and C57BL/6 mice was shaved using clippers prior to dissection. Dorsal tissue was
608 removed, cut into thin (~5mm) strips, and embedded in room temperature OCT. OCT blocks
609 were placed on dry ice to freeze and subsequently stored at -80°C . Both sexes were used. All
610 animals were between 3 and 6 weeks in age and were fed standard, non-sterilized rodent chow.
611 No pathogens were identified in the regular health screenings conducted by facility staff. Mice
612 were housed with 1-5 animals per cage with bedding and enrichment using Ventilated Thoren

613 racks. Mice were euthanized using CO_2 inhalation (as per the AVMA Guidelines for the
614 Euthanasia of Animals: 2020 Edition), followed by cervical dislocation. Dissections were
615 performed with ethanol-sterilized tools.
616
617 **Fluorescence in situ hybridization and imaging**
618 Human and mouse tissues were processed identically. 30 µm tissue sections were
619 sectioned and mounted on slides using a Leica CM3050S cryostat. Tissues on slides were fixed
620 in 4% formaldehyde in 1X PBS for 20 mins. Following fixation, tissues were washed for 5 mins
621 in 1X PBS and then incubated in hybridization buffer (0.9 M NaCl, 20 mM Tris-HCl, 10%
622 formamide) containing 10 mg/mL lysozyme and FISH probes at 1 µg/µL for 2-3 hours at 47ºC in
623 the dark. Nucleotide sequences of FISH probes can be found in Table S1. After hybridization,
624 slides were incubated in wash buffer (0.9 M NaCl, 20 mM Tris-HCl) for 1 hr at 47ºC in the dark.
625 Slides were then washed in 1X PBS for 10 mins. To visualize tissue nuclei, tissues were then
626 stained with 1 µg/mL DAPI for 10 mins at room temperature. Slides were then washed 3X in 1X
627 PBS for 10 mins each. Following the final wash step, tissues were mounted with glycerol-based
628 anti-fade non-curing mounting media. Coverslips were sealed using a 1:1:1 mixture of petroleum
629 jelly, lanolin, and paraffin. Images were acquired on a Nikon A1R-Si HD confocal microscope
630 controlled by NIS Elements software. ImageJ and MATLAB (Mathworks, Natwick, MA) were
631 used for image processing. To calculate fluorescence enrichment scores, maximum projections
632 of Z-stacks were used. A rectangular region of interest (ROI) of width W was drawn around a
633 follicle using only the DAPI channel. A second ROI was drawn near the follicle opening with
634 dimensions 0.5W x 2W in order to capture follicle-associated fluorescence near the follicle
635 opening. In an orthogonal processing step, the pixel intensities for the entire image in the FISH

636 fluorescent channel were fit using a 3 component Gaussian mixture model (GMM)
637 corresponding roughly to non-tissue background, non-probe autofluorescence, and probe-based
638 signal. Using this GMM as the background subtraction value for each image, the mean intensity
639 for each ROI was calculated. This threshold value was used to calculate the mean fluorescence
640 value inside the ROI and outside the ROI. The ratio of the mean fluorescence value inside the
641 ROI to the mean fluorescence value outside of the ROI was used for quantifying follicle- and
642 stratum corneum-associated fluorescence (enrichment score). Significance was calculated using
643 the Mann-Whitney test.

644 Stationary phase cultures were grown according to the following conditions:

Strain	Growth time	Media	Environmental condition
Cutibacterium acnes ATCC6919	72 hours	Reinforced clostridial medium (RCM) (Oxoid, CM0149)	Anaerobic, 37ºC
Corynebacterium striatum ATCC6940	24 hours	Brain heart infusion (BHI) (BD, 237500)	Aerobic, 30ºC
Micrococcus luteus ATCC4698	24 hours	Tryptic soy broth (TSB) (BD, 211825)	Aerobic, 30ºC
Staphylococcus epidermidis EGM 2-06	24 hours	Tryptic soy broth (TSB) (BD, 211825)	Aerobic, 37ºC

645

646 **Human subject microbiome samples**

647 Microbiome samples were collected under Princeton University IRB #13003 at the
648 Princeton University Department of Molecular Biology. Healthy volunteers were recruited via
649 informational flyers. Volunteers gave informed consent prior to sample collection. Participants
650 were healthy volunteers, male and female, white, aged 26-35, with no history of chronic skin
651 conditions or autoimmune disease and were not using antibiotics at the time of sampling or one
652 month prior to sample collection.

653 Skin microbiomes from healthy volunteers were collected using sterile foam-tipped
654 collection swabs pre-moistened with sterile 1X DPBS. Though often included, we chose not to
655 use detergent in the swabbing buffer in order to avoid negatively affecting bacterial cell
656 membranes and altering viability scores. Figure 2 – figure supplement 1G shows how swabbing
657 with and without 0.1% Triton X-100 (Sigma) affects viability scores, ddPCR results, and CFU.
658 Areas of interest were sampled for 60 seconds before being re-suspended in sterile 1X DPBS.
659 Tongue microbiome samples were collected using sterile foam-tipped collection swabs. Hair
660 shaft samples were collected by plucking hairs and using only the bulb portion. Follicle contents
661 were collected using Bioré Deep Cleansing Pore Strips (Kao USA Inc., Cincinnati, OH). Saliva
662 was collected in sterile 50 mL conicals from healthy volunteers. Plaque was collected by
663 scraping the teeth of healthy volunteers using sterile toothpicks and re-suspending the collection
664 in sterile 1X DPBS. Murine fecal samples from C57BL/6 mice were collected during dissection.
665 Human skin microbiome samples shown in Figure 2 – figure supplement 1 were plated for CFU
666 calculations prior to the addition of PMA. Samples were plated on blood agar plates (5% sheep
667 blood in tryptic soy agar, VWR International) and grown for 24-48 hours aerobically or
668 anaerobically. For perturbation recovery experiments, volunteers were asked to refrain from
669 using any type of products on their face for the duration of the experiment (48 hours) as well as
670 24 hours prior to baseline sampling. Volunteers were allowed to bathe/shower, but were asked to
671 refrain from washing their faces. Skin surface sterilization was done by scrubbing the sample
672 area for 60 seconds with an antiseptic wipe containing benzalkonium chloride 0.13% w/v (North
673 by Honeywell, #150910). To ensure that the process of sampling the skin surface would not
674 affect the bacterial repopulation dynamics, forehead of each volunteer into four sections of equal
675 areas: T0 (baseline, before sterilization), T1 (3hrs post sterilization), T2 (24 hrs post-

676 sterilization), and T3 (48 hrs post-sterilization). Each section was sampled for 60 seconds using a
677 sterile foam-tipped collection swab pre-moistened with sterile 1X DPBS. As described above,
678 each swab was then resuspended in sterile 1X DPBS.
679 The human fecal sample was collected by the Donia lab under Princeton University IRB
680 #11606 and was gifted to the Gitai lab. This sample and the methods of collection were
681 described in Javdan, Bahar et al. "Personalized Mapping of Drug Metabolism by the Human Gut
682 Microbiome." *Cell* vol. 181,7 (2020): 1661-1679.e22. doi:10.1016/j.cell.2020.05.001 (*27*).
683
684 **Heat-killed *E. coli* ratios**
685 In order to demonstrate the efficacy of PMA, known ratios of live and heat-killed *E. coli* cultures
686 were mixed and subjected to PMA treatment. First, an overnight culture of *E. coli* NCM3722
687 was back-diluted into fresh LB media at a ratio of 1:1000 and grown at 37°C for 4 hours to reach
688 mid-log. Stationary-phase experiments were done with overnight, 18h cultures. Cultures were
689 then washed 3X and suspended in sterile PBS. Half of the culture was heat-killed by incubating
690 at 70°C for 20 minutes while the other half remained at room temperature. The heat-killed *E. coli*
691 cultures were allowed to cool to room temperature before combining with non-heat-killed *E. coli*
692 cultures to achieve a 50% (by volume) heat-killed mixture. For the 0% heat-killed, no heat-killed
693 bacteria were added. Likewise, for the 100% heat-killed, only heat-killed bacteria were used.
694 Each condition was mixed well and then split evenly between two sterile 1.5 mL microcentrifuge
695 tubes.
696
697 **Propidium monoazide (PMA) treatment, DNA isolation**

698 After collection, samples were split evenly between two sterile 1.5 mL microcentrifuge
699 tubes. PMA (Biotium Inc.) was added to one of the two tubes to a final concentration of 50 µM.
700 All tubes were incubated in the dark at room temperature for 10 mins before being exposed to
701 light to cross-link PMA molecules using the PMA-Lite™ LED Photolysis Device (Biotium Inc.).
702 DNA was then isolated from all samples using either the DNeasy PowerSoil Kit (Qiagen) or
703 according to the protocol outlined in Meisel et al. (*28*). The Meisel et al. protocol was modified
704 such that sonication (Branson Sonifier 250, VWR Scientific) was used instead of bead-beating
705 for the purposes of cell-lysis. Both DNA isolation methods work similarly (Figure 2 – figure
706 supplement 1H). If lysostaphin (Sigma-Aldrich) was used, it was added following PMA
707 activation and before DNA isolation to a final concentration of 0.1 mg/mL and incubated at room
708 temperature for 30 mins.
709
710 **Droplet digital PCR (ddPCR)**
711 The Bio Rad QX200 AutoDG Droplet Digital PCR System was used to quantify
712 extracted DNA from microbiome samples and from pure bacterial cultures. Reaction mixtures
713 contained 2x QX200 ddPCR EvaGreen Supermix and universal 16S qPCR primers at 10 nM
714 concentrations in a total volume of 25 µL. Primer sequences can be found in Table S1. Reaction
715 mixtures were transferred to sterile ddPCR 96-well plates (BioRad #12001925) which were
716 loaded into the QX200 Automated Droplet Generator. After droplet generation, the plate was
717 heat-sealed using the PX1 PCR Plate Sealer (BioRad #1814000) and PCR was performed with a
718 pre-step of 95 C for 5 minutes followed by 40 rounds of amplification with 60C, 1 minute
719 extensions and a final hold temperature of 12 C using a C1000 Touch Thermal Cycler (BioRad
720 #1851197). Samples were subsequently loaded into the QX200 Droplet Reader for

721 quantification. Automatic thresholding was performed using the Quantasoft software and
722 subsequently exported to Microsoft Excel for analysis. Significance was calculated using a
723 Student's T-Test. To calculate the viability score for a given pair of "-PMA" and "+PMA"
724 matched samples, the following calculation was done:
725

726 $$\frac{Copies\ per\ 20\ \mu L\ with\ PMA}{Copies\ per\ 20\ \mu L\ without\ PMA}$$

727

728 **ddPCR and CFU standard curves**

729 Cultures of *S. epidermidis* EGM 2-06 were grown in tryptic soy broth (TSB) overnight
730 and diluted 1:1000 the following morning in TSB and grown for 4 hours until a final OD of 0.4.
731 Tenfold dilutions of *S. epidermidis* culture were then prepared, plated for CFU on 5% sheep
732 blood in tryptic soy agar (VWR International) and divided between two 1.5 mL microcentrifuge
733 tubes. Stationary-phase cultures of *C. acnes, S. epidermidis, M. luteus,* and *C. striatum* were
734 grown according to the table above. PMA was added to one tube for a final concentration of 50
735 µM and the other tube was left untreated. PMA activation and DNA isolation was then done
736 according to the methods outlined above.
737

738 **16S rRNA gene amplicon sequencing**

739 DNA was isolated from microbiome samples (with and without PMA) using the DNeasy
740 PowerSoil Kit (Qiagen) (Figures 2-5) or according to the protocol outlined in Meisel et al
741 (Figure 6). The V1-V3 region of the 16S gene was amplified using the primers 27F (5'-
742 AGAGTTTGATCCTGGCTCAG) and 534R (5'- ATTACCGCGGCTGCTGG). Illumina
743 sequencing libraries were prepared using previously published primers (*29*). Libraries were then

744 pooled at equimolar ratios and sequenced on an Illumina MiSeq Micro 500 nt (Figure 3, Figure
745 4) or MiSeq V3 600 nt (Figure 6) as paired-end reads. Reads were 2X250 bp or 2X300 bp with
746 an average depth of ~33,616 reads for 500 nt and 245,488 reads for 600 nt (Tables S2, S3). Also
747 included were 8 bp Index reads, following the manufacturer's protocol (Illumina, USA). Raw
748 sequencing reads were filtered by Illumina HiSeq Control Software to generate Pass-Filter reads
749 for further analysis. Index reads were used for sample de-multiplexing. Amplicon sequencing
750 variants (ASVs) were then inferred from the sequences using the DADA2 plugin within QIIME2
751 version 2018.6 (*30*, *31*). Reverse reads were trimmed to 245 bp for the 2X250 bp data, and the
752 reverse reads were trimmed to 275 bp for the 2X300 bp data. For the 2X250 bp data, two
753 different ASV inference methods were utilized: one using only the forward reads (to capture the
754 longer-than-average Staphylococcus amplicons) and one using both paired-end reads. For the
755 2X300 bp data, ASV inference was performed using both paired-end reads. ASV inference using
756 forward reads was performed using DADA2's denoise-single function ,while ASV inference
757 using both reads was performed using the denoise-paired function.. Taxonomy was assigned to
758 the resulting ASVs with a naive Bayes classifier trained on the GreenGenes database version
759 using only the regions of the 16S rRNA gene spanned by the ASVs (*32*, *33*). All downstream
760 analyses were performed using family-level taxonomy assignments unless specified to be at the
761 ASV-level. PBS control samples were included at the library preparation step for 500 nt
762 sequencing data and air swab DNA isolation controls were included for 600 nt sequencing data.
763 Contamination removal was performed on 600 nt sequencing data using the Decontam package
764 for R (Figure 6 and Figure 6 – figure supplement 2 show data without contamination removal).
765 (*34*). Figure 6 – figure supplement 3 shows how Shannon diversity and richness change between
766 traditional sequencing and PMA-seq (similar to what is shown in Figure 3B and Figure 3C).

767 Removal of contaminants (using either 0.1 or 0.2 threshold) has little effect on the data,
768 suggesting that, although contamination removal cannot be performed on the 500 nt sequencing
769 data due to the absence of air swab controls, this should not change the overall findings shown in
770 Figure 3 and Figure 4. Relative abundance, richness, Shannon diversity, Bray-Curtis
771 dissimilarity, and PMA-index were assessed using the Vegan package for R or Microsoft Excel
772 and plotted using R, Prism, and MATLAB (*35*). The PMA-index was calculated using relative
773 abundance and was not calculated for any bacterial taxa that was present in fewer than four
774 samples.
775
776 **Data availability**
777 Sequencing datasets generated and analyzed during this study are available at NCBI Sequence
778 Read Archive (SRA) (BioProject numbers (PRINA918671 and PRINA918959). Oligonucleotide
779 sequences used are included in table S1.

780 **Acknowledgments:** We thank all members of the Gitai lab for their insights and comments. We
781 also thank Dr. Gary Laevsky and the Princeton Molecular Biology Microscopy Core, which is a
782 Nikon Center of Excellence, for microscopy support; Dr. Wei Wang and the Genomics Core
783 Facility in The Lewis Sigler Institute for Integrative Genomics at Princeton University for
784 support with 16S rRNA gene amplicon sequencing; Matthew Cahn for his assistance with
785 processing 16S rRNA gene amplicon sequencing data; Bahar Javdan for processing the human
786 fecal sample; Elizabeth Grice for support and feedback; and Laurice Flowers and Elizabeth Grice
787 for providing the *Staphylococcus epidermidis* strain used. **Funding:** Funding was provided in
788 part by NIH (DP1AI124669 to Z.G., E.M.A., and B.P.B., and T32 GM007388 to E.M.A).
789 Additional funding provided by the National Science Foundation (NSF PHY-1734030 to
790 B.P.B.). Research reported in this publication was also supported by the National Center for
791 Advancing Translational Sciences of the National Institutes of Health under Award Number
792 TL1TR003019 (E.M.A) and by the Schmidt Transformative Technology Fund (E.M.A.). This
793 work was supported in part by the Penn Skin Biology and Diseases Resource-based Center (P30-
794 AR068589) and the University of Pennsylvania Perelman School of Medicine. The contents are
795 solely the responsibility of the authors and do not necessarily represent the official views of the
796 respective funding agencies.

797 **References**

798 1. R. L. Gallo, Human Skin Is the Largest Epithelial Surface for Interaction with Microbes.
799 *J. Invest. Dermatol.* **137** (2017), pp. 1213–1214.
800 2. K. Maeda, New method of measurement of epidermal turnover in humans. *Cosmetics*
801 (2017), doi:10.3390/cosmetics4040047.
802 3. T. C. Scharschmidt, K. S. Vasquez, H. A. Truong, S. V. Gearty, M. L. Pauli, A. Nosbaum,
803 I. K. Gratz, M. Otto, J. J. Moon, J. Liese, A. K. Abbas, M. A. Fischbach, M. D.
804 Rosenblum, A Wave of Regulatory T Cells into Neonatal Skin Mediates Tolerance to
805 Commensal Microbes. *Immunity*. **43**, 1011–1021 (2015).
806 4. K. Polak-Witka, L. Rudnicka, U. Blume-Peytavi, A. Vogt, The role of the microbiome in
807 scalp hair follicle biology and disease. *Exp. Dermatol.* (2020), , doi:10.1111/exd.13935.
808 5. L. R. Kalan, J. S. Meisel, M. A. Loesche, J. Horwinski, I. Soaita, X. Chen, A. Uberoi, S.
809 E. Gardner, E. A. Grice, Strain- and Species-Level Variation in the Microbiome of
810 Diabetic Wounds Is Associated with Clinical Outcomes and Therapeutic Efficacy. *Cell*
811 *Host Microbe* (2019), doi:10.1016/j.chom.2019.03.006.
812 6. J. H. Kim, B. Yang, A. Tedesco, E. G. D. Lebig, P. M. Ruegger, K. Xu, J. Borneman, M.
813 Martins-Green, High Levels of Oxidative Stress and Skin Microbiome are Critical for
814 Initiation and Development of Chronic Wounds in Diabetic Mice. *Sci. Rep.* **9**, 1–16
815 (2019).
816 7. M. Loesche, S. E. Gardner, L. Kalan, J. Horwinski, Q. Zheng, B. P. Hodkinson, A. S.
817 Tyldsley, C. L. Franciscus, S. L. Hillis, S. Mehta, D. J. Margolis, E. A. Grice, Temporal
818 Stability in Chronic Wound Microbiota Is Associated With Poor Healing. *J. Invest.*
819 *Dermatol.* **137**, 237–244 (2017).

820 8. A. L. Byrd, Y. Belkaid, J. A. Segre, The human skin microbiome. *Nat. Rev. Microbiol.*
821 (2018), , doi:10.1038/nrmicro.2017.157.
822 9. J. S. Meisel, G. Sfyroera, C. Bartow-McKenney, C. Gimblet, J. Bugayev, J. Horwinski, B.
823 Kim, J. R. Brestoff, A. S. Tyldsley, Q. Zheng, B. P. Hodkinson, D. Artis, E. A. Grice,
824 Commensal microbiota modulate gene expression in the skin. *Microbiome* (2018),
825 doi:10.1186/s40168-018-0404-9.
826 10. T. C. Scharschmidt, K. S. Vasquez, M. L. Pauli, E. G. Leitner, K. Chu, H. A. Truong, M.
827 M. Lowe, R. Sanchez Rodriguez, N. Ali, Z. G. Laszik, J. L. Sonnenburg, S. E. Millar, M.
828 D. Rosenblum, Commensal Microbes and Hair Follicle Morphogenesis Coordinately
829 Drive Treg Migration into Neonatal Skin. *Cell Host Microbe* (2017),
830 doi:10.1016/j.chom.2017.03.001.
831 11. M. C. Nielsen, S. C. Jiang, Alterations of the human skin microbiome after ocean water
832 exposure. *Mar. Pollut. Bull.* (2019), doi:10.1016/j.marpolbul.2019.06.047.
833 12. C. Huttenhower, D. Gevers, R. Knight, S. Abubucker, J. H. Badger, A. T. Chinwalla, H.
834 H. Creasy, A. M. Earl, M. G. Fitzgerald, R. S. Fulton, M. G. Giglio, K. Hallsworth-Pepin,
835 E. A. Lobos, R. Madupu, V. Magrini, J. C. Martin, M. Mitreva, D. M. Muzny, E. J.
836 Sodergren, J. Versalovic, A. M. Wollam, K. C. Worley, J. R. Wortman, S. K. Young, Q.
837 Zeng, K. M. Aagaard, O. O. Abolude, E. Allen-Vercoe, E. J. Alm, L. Alvarado, G. L.
838 Andersen, S. Anderson, E. Appelbaum, H. M. Arachchi, G. Armitage, C. A. Arze, T.
839 Ayvaz, C. C. Baker, L. Begg, T. Belachew, V. Bhonagiri, M. Bihan, M. J. Blaser, T.
840 Bloom, V. Bonazzi, J. Paul Brooks, G. A. Buck, C. J. Buhay, D. A. Busam, J. L.
841 Campbell, S. R. Canon, B. L. Cantarel, P. S. G. Chain, I. M. A. Chen, L. Chen, S.
842 Chhibba, K. Chu, D. M. Ciulla, J. C. Clemente, S. W. Clifton, S. Conlan, J. Crabtree, M.

A. Cutting, N. J. Davidovics, C. C. Davis, T. Z. Desantis, C. Deal, K. D. Delehaunty, F. E. Dewhirst, E. Deych, Y. Ding, D. J. Dooling, S. P. Dugan, W. Michael Dunne, A. Scott Durkin, R. C. Edgar, R. L. Erlich, C. N. Farmer, R. M. Farrell, K. Faust, M. Feldgarden, V. M. Felix, S. Fisher, A. A. Fodor, L. J. Forney, L. Foster, V. Di Francesco, J. Friedman, D. C. Friedrich, C. C. Fronick, L. L. Fulton, H. Gao, N. Garcia, G. Giannoukos, C. Giblin, M. Y. Giovanni, J. M. Goldberg, J. Goll, A. Gonzalez, A. Griggs, S. Gujja, S. Kinder Haake, B. J. Haas, H. A. Hamilton, E. L. Harris, T. A. Hepburn, B. Herter, D. E. Hoffmann, M. E. Holder, C. Howarth, K. H. Huang, S. M. Huse, J. Izard, J. K. Jansson, H. Jiang, C. Jordan, V. Joshi, J. A. Katancik, W. A. Keitel, S. T. Kelley, C. Kells, N. B. King, D. Knights, H. H. Kong, O. Koren, S. Koren, K. C. Kota, C. L. Kovar, N. C. Kyrpides, P. S. La Rosa, S. L. Lee, K. P. Lemon, N. Lennon, C. M. Lewis, L. Lewis, R. E. Ley, K. Li, K. Liolios, B. Liu, Y. Liu, C. C. Lo, C. A. Lozupone, R. Dwayne Lunsford, T. Madden, A. A. Mahurkar, P. J. Mannon, E. R. Mardis, V. M. Markowitz, K. Mavromatis, J. M. McCorrison, D. McDonald, J. McEwen, A. L. McGuire, P. McInnes, T. Mehta, K. A. Mihindukulasuriya, J. R. Miller, P. J. Minx, I. Newsham, C. Nusbaum, M. Oglaughlin, J. Orvis, I. Pagani, K. Palaniappan, S. M. Patel, M. Pearson, J. Peterson, M. Podar, C. Pohl, K. S. Pollard, M. Pop, M. E. Priest, L. M. Proctor, X. Qin, J. Raes, J. Ravel, J. G. Reid, M. Rho, R. Rhodes, K. P. Riehle, M. C. Rivera, B. Rodriguez-Mueller, Y. H. Rogers, M. C. Ross, C. Russ, R. K. Sanka, P. Sankar, J. Fah Sathirapongsasuti, J. A. Schloss, P. D. Schloss, T. M. Schmidt, M. Scholz, L. Schriml, A. M. Schubert, N. Segata, J. A. Segre, W. D. Shannon, R. R. Sharp, T. J. Sharpton, N. Shenoy, N. U. Sheth, G. A. Simone, I. Singh, C. S. Smillie, J. D. Sobel, D. D. Sommer, P. Spicer, G. G. Sutton, S. M. Sykes, D. G. Tabbaa, M. Thiagarajan, C. M. Tomlinson, M. Torralba, T. J. Treangen, R. M. Truty,

866 T. A. Vishnivetskaya, J. Walker, L. Wang, Z. Wang, D. V. Ward, W. Warren, M. A.
867 Watson, C. Wellington, K. A. Wetterstrand, J. R. White, K. Wilczek-Boney, Y. Wu, K.
868 M. Wylie, T. Wylie, C. Yandava, L. Ye, Y. Ye, S. Yooseph, B. P. Youmans, L. Zhang, Y.
869 Zhou, Y. Zhu, L. Zoloth, J. D. Zucker, B. W. Birren, R. A. Gibbs, S. K. Highlander, B. A.
870 Methé, K. E. Nelson, J. F. Petrosino, G. M. Weinstock, R. K. Wilson, O. White, Structure,
871 function and diversity of the healthy human microbiome. *Nature* (2012),
872 doi:10.1038/nature11234.
873 13. E. A. Grice, J. A. Segre, The skin microbiome. *Nat. Rev. Microbiol.* (2011), ,
874 doi:10.1038/nrmicro2537.
875 14. Y. Belkaid, S. Tamoutounour, The influence of skin microorganisms on cutaneous
876 immunity. *Nat. Rev. Immunol.* (2016), , doi:10.1038/nri.2016.48.
877 15. M. B. Lousada, T. Lachnit, J. Edelkamp, T. Rouillé, D. Ajdic, Y. Uchida, A. Di Nardo, T.
878 C. G. Bosch, R. Paus, Exploring the human hair follicle microbiome*. *Br. J. Dermatol.*
879 (2021), , doi:10.1111/bjd.19461.
880 16. R. I. Amann, B. J. Binder, R. J. Olson, S. W. Chisholm, R. Devereux, D. A. Stahl',
881 "Combination of 16S rRNA-Targeted Oligonucleotide Probes with Flow Cytometry for
882 Analyzing Mixed Microbial Populations" (1990).
883 17. R. D. Bjerre, L. W. Hugerth, F. Boulund, M. Seifert, J. D. Johansen, L. Engstrand, Effects
884 of sampling strategy and DNA extraction on human skin microbiome investigations. *Sci.*
885 *Rep.* **9**, 1–11 (2019).
886 18. A. Nocker, C. Y. Cheung, A. K. Camper, Comparison of propidium monoazide with
887 ethidium monoazide for differentiation of live vs. dead bacteria by selective removal of
888 DNA from dead cells. *J. Microbiol. Methods*. **67**, 310–320 (2006).

889 19. Y. Yang, D. Cheng, Y. Li, L. Yu, K. Y. H. Gin, J. P. Chen, M. Reinhard, Effects of
890 monochloramine and hydrogen peroxide on the bacterial community shifts in biologically
891 treated wastewater. *Chemosphere* (2017), doi:10.1016/j.chemosphere.2017.09.087.
892 20. A. Nocker, T. Richter-Heitmann, R. Montijn, F. Schuren, R. Kort, Discrimination between
893 live and dead cells in bacterial communities from environmental water samples analyzed
894 by 454 pyrosequencing. *Int. Microbiol.* (2010), doi:10.2436/20.1501.01.111.
895 21. S. F. Stoddard, B. J. Smith, R. Hein, B. R. K. Roller, T. M. Schmidt, rrnDB: improved
896 tools for interpreting rRNA gene abundance in bacteria and archaea and a new foundation
897 for future development. *Nucleic Acids Res.* **43**, D593–D598 (2015).
898 22. Q. Liu, Q. Liu, H. Meng, H. Lv, Y. Liu, J. Liu, H. Wang, L. He, J. Qin, Y. Wang, Y. Dai,
899 M. Otto, M. Li, Staphylococcus epidermidis Contributes to Healthy Maturation of the
900 Nasal Microbiome by Stimulating Antimicrobial Peptide Production. *Cell Host Microbe*.
901 **27**, 68-78.e5 (2020).
902 23. J. Oh, A. L. Byrd, M. Park, H. H. Kong, J. A. Segre, Temporal Stability of the Human
903 Skin Microbiome. *Cell* (2016), doi:10.1016/j.cell.2016.04.008.
904 24. Y. Yu, S. Dunaway, J. Champer, J. Kim, A. Alikhan, Changing our microbiome:
905 probiotics in dermatology. *Br. J. Dermatol.* (2020), , doi:10.1111/bjd.18088.
906 25. A. Conwill, A. C. Kuan, R. Damerla, A. J. Poret, J. S. Baker, A. D. Tripp, E. J. Alm, T. D.
907 Lieberman, Anatomy promotes neutral coexistence of strains in the human skin
908 microbiome. *Cell Host Microbe*. **30**, 171-182.e7 (2022).
909 26. W. Van'T Hof, E. C. I. Veerman, A. V. N. Amerongen, A. J. M. Ligtenberg,
910 Antimicrobial defense systems in saliva. *Monogr. Oral Sci.* (2014),
911 doi:10.1159/000358783.

912 27. B. Javdan, J. G. Lopez, P. Chankhamjon, Y. C. J. Lee, R. Hull, Q. Wu, X. Wang, S.
913 Chatterjee, M. S. Donia, Personalized Mapping of Drug Metabolism by the Human Gut
914 Microbiome. *Cell*. **181**, 1661-1679.e22 (2020).
915 28. J. S. Meisel, G. D. Hannigan, A. S. Tyldsley, A. J. SanMiguel, B. P. Hodkinson, Q.
916 Zheng, E. A. Grice, Skin Microbiome Surveys Are Strongly Influenced by Experimental
917 Design. *J. Invest. Dermatol.* (2016), doi:10.1016/j.jid.2016.01.016.
918 29. J. G. Caporaso, C. L. Lauber, W. A. Walters, D. Berg-Lyons, J. Huntley, N. Fierer, S. M.
919 Owens, J. Betley, L. Fraser, M. Bauer, N. Gormley, J. A. Gilbert, G. Smith, R. Knight,
920 Ultra-high-throughput microbial community analysis on the Illumina HiSeq and MiSeq
921 platforms. *ISME J.* (2012), doi:10.1038/ismej.2012.8.
922 30. E. Bolyen, J. R. Rideout, M. Dillon, N. Bokulich, C. Abnet, G. Al-Ghalith, H. Alexander,
923 E. Alm, M. Arumugam, F. Asnicar, Y. Bai, J. Bisanz, K. Bittinger, A. Brejnrod, C.
924 Brislawn, C. T. Brown, B. Callahan, A. M. Caraballo-Rodríguez, J. Chase, E. Cope, R. Da
925 Silva, P. Dorrestein, G. Douglas, D. Durall, C. Duvallet, C. Edwardson, M. Ernst, M.
926 Estaki, J. Fouquier, J. Gauglitz, D. Gibson, A. Gonzalez, K. Gorlick, J. Guo, B. Hillmann,
927 S. Holmes, H. Holste, C. Huttenhower, G. Huttley, S. Janssen, A. Jarmusch, L. Jiang, B.
928 Kaehler, K. Bin Kang, C. Keefe, P. Keim, S. Kelley, D. Knights, I. Koester, T. Kosciolek,
929 J. Kreps, M. G. Langille, J. Lee, R. Ley, Y.-X. Liu, E. Loftfield, C. Lozupone, M. Maher,
930 C. Marotz, B. Martin, D. McDonald, L. McIver, A. Melnik, J. Metcalf, S. Morgan, J.
931 Morton, A. T. Naimey, J. Navas-Molina, L. F. Nothias, S. Orchanian, T. Pearson, S.
932 Peoples, D. Petras, M. L. Preuss, E. Pruesse, L. B. Rasmussen, A. Rivers, M. Robeson, II,
933 P. Rosenthal, N. Segata, M. Shaffer, A. Shiffer, R. Sinha, S. J. Song, J. Spear, A.
934 Swafford, L. Thompson, P. Torres, P. Trinh, A. Tripathi, P. Turnbaugh, S. Ul-Hasan, J. J.

935 van der Hooft, F. Vargas, Y. Vázquez-Baeza, E. Vogtmann, M. von Hippel, W. Walters,
936 Y. Wan, M. Wang, J. Warren, K. Weber, C. H. Williamson, A. Willis, Z. Z. Xu, J.
937 Zaneveld, Y. Zhang, Q. Zhu, R. Knight, J. G. Caporaso, QIIME 2: Reproducible,
938 interactive, scalable, and extensible microbiome data science. *PeerJ* (2018),
939 doi:10.7287/peerj.preprints.27295.
940 31. B. J. Callahan, P. J. McMurdie, M. J. Rosen, A. W. Han, A. J. A. Johnson, S. P. Holmes,
941 DADA2: High-resolution sample inference from Illumina amplicon data. *Nat. Methods*
942 (2016), doi:10.1038/nmeth.3869.
943 32. N. A. Bokulich, B. D. Kaehler, J. R. Rideout, M. Dillon, E. Bolyen, R. Knight, G. A.
944 Huttley, J. Gregory Caporaso, Optimizing taxonomic classification of marker-gene
945 amplicon sequences with QIIME 2's q2-feature-classifier plugin. *Microbiome* (2018),
946 doi:10.1186/s40168-018-0470-z.
947 33. D. McDonald, M. N. Price, J. Goodrich, E. P. Nawrocki, T. Z. Desantis, A. Probst, G. L.
948 Andersen, R. Knight, P. Hugenholtz, An improved Greengenes taxonomy with explicit
949 ranks for ecological and evolutionary analyses of bacteria and archaea. *ISME J.* (2012),
950 doi:10.1038/ismej.2011.139.
951 34. N. M. Davis, Di. M. Proctor, S. P. Holmes, D. A. Relman, B. J. Callahan, Simple
952 statistical identification and removal of contaminant sequences in marker-gene and
953 metagenomics data. *Microbiome*. **6**, 1–14 (2018).
954 35. J. Oksanen, F. G. Blanchet, M. Friendly, R. Kindt, P. Legendre, D. Mcglinn, P. R.
955 Minchin, R. B. O'Hara, G. L. Simpson, P. Solymos, M. H. H. Stevens, E. Szoecs, H.
956 Wagner, vegan: Community Ecology Package. R package version 2.4-2. *Community Ecol.*
957 *Packag.* (2019).